Article:
Dong, G., Hajirasouliha, I. orcid.org/0000-0003-2597-8200, Pilakoutas, K. orcid.org/0000-0001-6672-7665 et al. (1 more author) (2023) Multi-level performance-based seismic design optimisation of RC frames. Engineering Structures, 293. 116591. ISSN: 0141-0296

https://doi.org/10.1016/j.engstruct.2023.116591

Engineering Structures 293 (2023) 116591

Contents lists available at ScienceDirect

Engineering Structures

journal homepage: www.elsevier.com/locate/engstruct

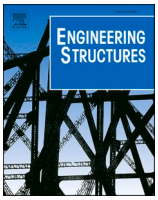

Multi-level performance-based seismic design optimisation of RC frames

Geyu Dong [a,*], Iman Hajirasouliha [a], Kypros Pilakoutas [a], Payam Asadi [b]

[a] Department of Civil and Structural Engineering, The University of Sheffield, Sheffield, UK
[b] Department of Civil Engineering, Isfahan University of Technology, 8415683111 Isfahan, Iran

ARTICLE INFO

Keywords:
Structural optimisation
Reinforced concrete frames
Multi-level performance based design
Global damage index
Nonlinear dynamic analyses

ABSTRACT

Conventional structural optimisation techniques often result in unconventional structural configurations, unrealistic structural elements and ignore actual construction costs. This paper presents an effective performance-based optimisation framework for minimising initial material costs of realistic multi-storey reinforced concrete (RC) frames, while satisfying pre-determined performance targets under multiple seismic hazard levels as well as a set of practical design and construction constraints. A new low computational-cost optimisation method is proposed to directly control specific response parameters at both the element and structural levels (i.e. plastic rotation and inter-storey drift). For the first time, the concept of Uniform Damage Distribution (UDD) is adopted to simplify the complex design optimisation problem of RC buildings with multiple design variables in terms of section sizes and reinforcement ratios. The optimum design solution is achieved by gradually redistributing materials from strong to weak parts of the structure, aiming to fully exploit the material capacity. The efficiency of the proposed optimisation framework is then demonstrated in the optimum designs of 3-, 5-, 10- and 15-storey RC frames under a set of six spectrum-compatible earthquake records. The results indicate that compared to structures designed by current codes, optimum solutions required up to 20 % and 43 % less concrete volume and steel reinforcement weight, respectively. It is also noted that due to more efficient use of materials, optimum structures exhibited considerably lower global damage index (up to 88 %), less maximum inter-storey drift (up to 58 %), and less maximum plastic rotations (up to 78 %). Sensitivity analysis on earthquake record selection shows that using a single earthquake record may not lead to reliable design solutions, in particular for tall buildings, and hence a set of spectrum-compatible records should be used in the optimisation process. This research will lead to more economical and safe design of multi-storey RC structures in seismic regions by developing a practical multi-level optimisation method with low computational costs.

1. Introduction

Current seismic design guidelines (e.g. Eurocode 8, Chinese code GB 50011, IBC 2021 [1–3]) generally adopt “strength-based” or “force-based” design principles. While these methods mainly ensure overall structural capacity, they cannot directly control member deformations and lateral drifts and in turn efficiently limit structural and non-structural damage under earthquakes. Moreover, most seismic design codes mainly aim to satisfy “life safety” requirements under design-basis earthquake (DBE) level (10 % probability of exceedance in 50 years) and, hence, may not satisfy target performance objectives under other seismic hazard levels. It should be noted that, structures designed using modern codes successfully protected occupants’ lives in recent major earthquake events (e.g. Christchurch 2010–2011, Northern Italy 2012, Kumamoto 2016); however, economic losses due to repairable and non-repairable damage were extremely large in some cases [4–6].

In current seismic design codes, the equivalent static lateral force determined to simulate seismic loads is based on the dynamic behaviour of linear elastic systems. However, typical RC structures do not generally remain elastic under severe earthquake events. In conventional seismic design approaches, structural nonlinearity and hysteretic energy dissipation capacity are generally taken into account by using a response modification factor (e.g. ASCE41 [7]) or a behaviour factor (e.g. Eurocode8 [1]). These factors are normally decided based on judgment and empirical evidence, and do not necessarily lead to most suitable design solutions, which is also confirmed by results from previous experimental and numerical studies [8,9]. On the other hand, while push-over analyses suggested in current seismic design guidelines aim to provide better predictions of structural seismic responses, previous studies have identified that: (i) the fixed load patter used in the pushover analysis

* Corresponding author.
E-mail address: gdong1@sheffield.ac.uk (G. Dong).

https://doi.org/10.1016/j.engstruct.2023.116591
Received 12 April 2023; Received in revised form 27 June 2023; Accepted 9 July 2023
Available online 18 July 2023

may be unrealistic when lateral inertia loads and storey stiffness change due to the occurrence of yielding and nonlinear structural behaviour; and (ii) the push-over analysis does not directly account the contribution of higher modes on structural behaviour, which can be especially important for high-rise buildings [10,11]. The study by [12] indicated that using a single pushover analysis cannot duplicate the interaction between the continuously changing dynamic characteristics of inelastic structural system with the various frequencies of earthquake records.

Performance-based design (PBD) has been introduced in more recent seismic resistant design guidelines (e.g. ATC-40, FEMA356, ASCE 41 [7,13,14]) and is intended to address some of the limitations of the conventional "force-based" design methods [15,16]. In PBD, a set of design criteria are expressed in terms of performance objectives that directly correspond to specific requirements for the building (i.e. immediate occupancy, life safety, collapse prevention) under different seismic hazard levels. This provides a more direct and rational approach for controlling structural and non-structural damage during the seismic design process. Mergos [17] compared to conventional design solutions (e.g. Eurocode 8 force-based design methods) subjected to earthquakes with different hazard levels. It was found that in several cases they failed to satisfy performance constraints on element plastic hinge rotations set by performance-based design criteria (e.g. MC2010). Though it is accepted that PBD can provide better control of structural damage during seismic events, it still does not necessarily guarantee the most efficient design.

The concept of "optimal design" has been widely utilised for different structural systems. For instance, Foraboschi [18] searched for the best thickness of the glass layers and the stillness of the interlayer to optimise the cost of plates made of glass, while fulfilling strength and deflection design requirements. In another study Domenico and Hajirasouliha [19] aimed to minimise structural damage of steel frames with nonlinear viscous dampers by remodifying damping coefficients of the dampers. RC frames are the most common structural system used worldwide for low and medium rise buildings. Even though, their overall structural design is relatively straight forward, obtaining their optimum design solution can be very challenging due to cracking of concrete affecting the lateral stiffness and inertia load distribution, as well as the nonlinear behaviour of the structure mainly caused by the yielding of reinforcement.

Several design optimisation studies on RC frames have been published in the past 20 years. Chan and Zou [19] and Zou et al. [20] aimed to obtain the optimum design of RC frames by employing an Optimality Criteria (OC) performance-based methodology. Both section sizes and steel reinforcement quantities were considered as design variables and optimised based on the performance results of elastic and inelastic (push-over) analyses, respectively. To achieve the optimum solution, objective functions subject to design constraints were first converted into an unconstrained Lagrangian function, and then the stationary condition of the Lagrangian function was evaluated. In another study, Bai et al. [21] developed an optimisation technique based on the concept of Optimality Criteria (OC) to achieve more uniform distribution of storey drifts. Inelastic response demands were evaluated through consecutive pushover analysis. Reinforcement areas of beams and columns were iteratively modified in accordance with storey lateral drifts and element hinge rotations, simultaneously. Furthermore, Liu et al. [22] used a second-order optimisation method for elastic seismic drift design of RC frames. This required to first transfer a constrained problem into an unconstrained optimisation formulation through an interior penalty function. Subsequently, the first and second derivatives of the penalty function were calculated to achieve seismic design with minimum structural weight. Dimensions of beams and columns were considered as the only design variables in the objective function. In a more recent study, Papazafeiropoulos et al. [23] used a gradient-based first-order optimisation methodology to achieve uniform distribution of dissipated energy for RC frames by optimising the distribution of structural stiffness.

Recently, evolutionary algorithms such as Genetic Algorithm (GA) and Evolution Strategies (ES) are also used in seismic design optimisation of RC frames [24–27]. Mergos [17,28] utilised GA in the optimum seismic design of RC frames in accordance with both force-based and performance-based design methods to minimise material costs. Section dimensions, diameter and number of longitudinal reinforcement bars, and diameter and number of transverse reinforcement bars were considered as design variables and were independently remodified according to a set of design constraints. In another study, Mitropoulou et al. [29] applied ES for multi-objective optimisation. To assess structural performance, both nonlinear static and dynamic analyses were conducted, while discrete design variables including dimensions of members, longitudinal and transverse steel reinforcements were considered. Razmara Shooli et al. [30] also adopted a mixed GA and Particle Swarm Optimisation (PSO) in conjunction with nonlinear static and dynamic analysis methods for PBD optimisation of RC frames. Their optimisation method was first processed with nonlinear static analyses to obtain the optimum search domain involving specific design variables, and then nonlinear dynamic analyses were performed to find the optimum result with minimum material cost within the identified search domain. Gholizadeh et at. [31] performed a reliability-based design optimisation of RC frames, where a Chaotic Enhanced Colliding Bodies Optimisation (CECBO) metaheuristic algorithm in conjunction with a metamodel was adopted to search for optimum solutions in a specific design space. In another relevant study, Razavi et al. [32] utilised the Improved Black Hole (IBH) metaheuristic algorithm to minimise initial cost and total life-cycle cost, as two different independent optimisation objectives. Specific design variables were optimised by using predetermined databases and based on seismic responses obtained from pushover analysis.

In general, the above-mentioned optimisation methodologies can be classified into two categories: (i) mathematical programming algorithms such as OC method and gradient-based algorithms and (ii) search-based optimisation methodologies including GA, ES and PSO. Most previous optimisation studies on RC frames adopting math-based algorithms required complex mathematical formulas to transfer inequality constraints and objective functions into unconstrained problems. They also required a high computational effort to calculate the derivatives of the objective functions at each optimisation step, particularly in the case of nonlinear systems under dynamic loads. Search-based design optimisation methods are also computationally expensive (i.e. require thousands of analysis iterations), while their optimisation speed and accuracy depend on the pre-determined search domain. Moreover, more than half of previous optimisation studies adopted nonlinear static (pushover) analysis with predefined lateral load patterns to predict the seismic behaviour of structures. However, as mentioned before, using the fixed load patterns may not represent the actual seismic effects in a non-linear structural system. These limitations increase costs and limit accuracy, hence, may prevent engineers from using these optimisation methods in practical applications.

To reduce computational costs, Hajirasouliha et al. [33] developed a practical optimisation methodology for the seismic design of RC frames, based on the concept of Uniform Damage Distribution (UDD). Previous study demonstrated that this approach can significantly reduce the computational costs (up to 300 times less number of non-linear dynamic analysis) of the optimisation process of complex non-linear systems compared to the metaheuristics optimisation methods such as GA and PSO [34,35]. According to the design philosophy of UDD, structural materials are redistributed iteratively from low- to high-damaged areas until a state of nearly uniform height-wise distribution of structural damage is achieved. In follow-up studies, the UDD concept was adopted for the optimum seismic design of RC frames [36,37]. However, these studies mainly considered maximum inter-storey drift as the single performance index, which cannot comprehensively identify structural damage at both local and global levels. It should be noted that, the selection of performance levels plays an important role in performance-

Table 1
Relationship between performance objectives, corresponding seismic hazard level and peak ground acceleration.

Performance objective	Earthquake excitation	Occurrence Probability	Return Period (year)	PGA (g)
Immediate Occupancy (IO)	Frequent earthquake	50 % in 50 years	72	0.1
Life Safety (LS)	Design basis earthquake (DBE)	10 % in 50 years	475	0.4
Collapse Prevention (CP)	Maximum considered earthquake (MCE)	2 % in 50 years	2475	0.65

based optimisation methods. Previous optimisation studies using UDD, mainly considered a single performance objective (i.e. life safety) under a certain seismic hazard level (i.e. 10 % probability of exceedance in 50 years). This may not necessarily lead to a safe design solution in rarer earthquakes with higher intensity levels when high localised damage may develop [38].

In general, optimisation of RC frames is a complex problem since both reinforcement arrangement and weight, and concrete volume can significantly affect seismic responses of structures. Foraboschi [39] studied the bending load-carrying capacity of RC beams allowing for ductility, and concluded that a blending increasement in amount of reinforcement of the RC element does not compensate a reduction in its cross-section size. Indeed, many of the previous studies on the optimum design of RC frames only optimised the reinforcement ratios of the elements, while the initial dimensions were obtained based on existing seismic design guidelines and then kept unchanged during the optimisation process [33,21,40]. However, these two design variables are not independent, as structural ductility and deformability are affected by both parameters. On the other hand, Arroyo and Gutiérrez [27] and Arroyo et al. [41] mainly aimed to improve the elastic performance of the structural system by optimising the dimensions of the structural members, while the reinforcement bars were designed using current design codes after the optimisation stage. However, the optimum solution in this case may not guarantee the structural safety in future rare earthquakes, when structures are loaded beyond the elastic range.

The objective of this study is to develop an efficient multi-objective performance-based optimisation framework for seismic design of RC frames based on the concept of Uniform Damage Distribution (UDD). In this approach, the specific design variables change iteratively to closely approach the performance target limits. Consequently, material capacities in most storeys are to be fully exploited at least under one seismic hazard level, and hence a design solution with minimum material usage is obtained by satisfying all the performance targets corresponding to multiple design objectives. The novelty of the proposed framework is that, for the first time, the UDD approach is implemented to accommodate: (i) multi-level performance objectives under different seismic intensity levels ranging from elastic to inelastic states; (ii) optimising both section sizes and reinforcement ratios; and (iii) controlling both local (element plastic rotation) and global (inter-storey drift) performance indices simultaneously with low computational costs. The efficiency of the framework is demonstrated in the design of 3-, 5-, 10- and 15-storey RC frames under a set of spectrum-compatible earthquakes. The framework is further developed to investigate the effect of variability in the selected earthquake input records.

2. Performance-based optimisation framework

In this study, the optimisation objective is to minimise the total material usage (both concrete and reinforcement), while satisfying a set of performance constraints to control local and global structural damage under different earthquake intensity levels. This is achieved based on the concept of Uniform Damage Distribution (UDD), and by incorporating the design criteria in PBD. In accordance with ASCE 41-13 [7] recommendations and seismic hazard studies in several seismic source areas, Table 1 shows the performance objectives that should be satisfied in the multilevel performance-based optimisation, their corresponding seismic hazard levels (here expressed as occurrence probability of the earthquakes), and their relationship with magnitude of peak ground acceleration (PGA) for the design earthquakes used in the case studies [42,43].

2.1. Formulation of multi-objective optimum design problem

The design constraints on geometry and reinforcement detailing of beam and column elements are based on Eurocode 2 and 8 [1,44] recommendations for medium ductility level (DCM). Key practical design considerations adopted in common practice were also considered in the optimisation process. The overall optimisation problem can be expressed as:

$$Minimise:\ V_c,\ W_s$$

$$Subjected\ to:\ \theta_c \le \theta_{target,c}, .\theta_b \le \theta_{target,b}$$

$$\Delta_{max} \le \Delta_{target}$$

$$\rho_{c,min} \le \rho_c \le \rho_{c,max}$$

$$\rho_{b,min} \le \rho_{b,top} \le \rho_{b,max}$$

$$\rho_{b,min} \le \rho_{b,bottom} \le \rho_{b,max}$$

$$D_{min} \le D, B_{min} \le B, H_{min} \le H$$

where V_c is the total concrete volume in the frame, W_s is the total longitudinal reinforcement weights. θ_c and θ_b are plastic rotations of beams and columns, respectively. Δ_{max} denotes maximum inter-storey drift ratio. ρ_c is longitudinal reinforcement ratio of columns, while $\rho_{b,top}$ and $\rho_{b,bottom}$ are the ratio of beam top and bottom reinforcement, respectively. D is the dimension of column sections assumed to be square, and B and H are the width and depth of beam sections, respectively. The subscript "min" represents the minimum values of cross-section dimensions suggested by Eurocode. It should be noted that the optimisation framework proposed in this study is general and able to be adopted for any seismic design codes to obtain the most suitable design solution.

2.2. Design constraints

To achieve DCM in Eurocode 8, the minimum dimension of concrete sections is limited to 250 mm, and minimum and maximum reinforcement ratios in columns are 1 % and 4 %, respectively. Upper and lower reinforcement limits in beams are also imposed. To promote the "strong column/weak beam" design principle, at each beam-column joint the sum of the flexural stiffnesses of beams is designed to be less than the flexural stiffness of columns. Additionally, according to practical considerations from engineering experience, it is recommended that the width of beams should be always less than the dimensions of columns, and dimensions of columns shouldn't be less than the ones in upper storeys.

2.3. Design variables in UDD optimisation

As mentioned in the above problem formulation, this study aims to minimise both rebar weights (kg) and concrete volume (m^3) of RC frames. Column dimensions (D) as well as beam width (B) and depth (H) are accounted as discrete design variables, while longitudinal

Table 2
Column plastic rotation capacity ($\theta_{target,C}$)(unit: rad) (ASCE 41–13 [7]).

$\frac{P}{A_g f_c'}$	$\frac{V}{b_w d\sqrt{f_c'}}$	$\rho = \frac{A_v}{b_w s}$	Performance Level	
			LS	CP
≤ 0.1	≤ 3	≥ 0.006	0.045	0.060
≥ 0.6	≤ 3	≥ 0.006	0.009	0.010
≤ 0.1	≤ 3	≤ 0.0005	0.010	0.012
≥ 0.6	≤ 3	≤ 0.0005	0.003	0.004

Table 3
Beam plastic rotation capacity ($\theta_{target,B}$) (unit: rad) (ASCE 41–13 [7]).

$\frac{\rho - \rho'}{\rho_{bal}}$	$\frac{V_b}{b_w d\sqrt{f_c'}}$	Performance Level	
		LS	CP
≤ 0.0	≤ 3	0.025	0.050
≥ 0.5	≤ 3	0.020	0.030
≤ 0.0	≥ 6	0.020	0.040
≥ 0.5	≥ 6	0.015	0.020

reinforcement ratios in columns (ρ_c) and beams ($\rho_{b,top}$, $\rho_{b,bottom}$) are considered as continuous variables in the optimisation process. The proposed study assumes that each RC member has adequate amount of transverse reinforcement that is approximately proportional to the longitudinal reinforcement quantity. The values of all the selected design variables also satisfy the practical and code-based design constraints in each iterative step during the optimisation procedure.

2.4. Performance parameters and design targets

The current method considers plastic hinge rotations in beams (θ_b) and columns (θ_c) as primary performance parameters to measure local element response quantities under medium to severe earthquakes, while the inter-storey drifts (Δ_{max}), as more global performance parameters, are also simultaneously controlled in the optimisation process. It should be noted that the performance parameters in the proposed optimization methodology are selected based on the suggestions in ASCE 41. However, the adopted UDD method is general, and can be efficiently applied to any other performance parameters such as floor acceleration and velocity.

Axial load ratios and transverse reinforcements ratios are important parameters that affect the rotation capacity of RC elements under earthquake loads, while the flexural capacity is also influenced by shear loads [45]. Yuen et al. [46] shows that increasing axial load ratios reduces ductility and energy dissipation capacity of flexure-dominated columns. Therefore, the plastic hinge rotation target limit (capacity) cannot be pre-determined and should be updated following the section properties and loading information (i.e. shear load, axial load) at each iterative step of the optimisation procedure. This increases the complexity of the optimisation problem for RC frames under multiple earthquake intensity levels.

Once the target performance level is decided (e.g. IO, LS, CP), target limits (capacities) of plastic hinge rotation of beams ($\theta_{target,B}$) and columns ($\theta_{target,C}$) can be calculated following ASCE 41-13 guidelines as presented in Tables 2 and 3, respectively. In these tables: P is the column axial load, A_g is the column cross section area, f_c' is concrete compressive strength, V is design shear force in columns, b_w is section width, d is distance between compression rebar to centroid of tension reinforcement, A_v is shear reinforcement area, s is spacing of shear reinforcement, ρ is tension reinforcement ratio, ρ' is compression reinforcement ratio, ρ_{bal} is reinforcement ratio producing balanced strain conditions, and V_b is beam shear force.

To constrain performance at structural level, the target inter-storey drift ratios (Δ_{target}) are defined as 1 %, 2 % and 4 % at performance levels IO, LS and CP, respectively, in accordance with ASCE 41-06 [47].

It should be noted that, the proposed methodology is general and other drift limits can be easily adopted. To provide more accurate results, structural response parameters are obtained through non-linear time history analysis (NTHA) using OpenSees software [48]. The iterative optimisation process based on UDD concept is performed by a specifically designed subroutine in MATLAB [49].

2.5. Multi-level UDD optimisation

The seismic design of RC structures is commonly based on the assumption that the buildings experience nearly elastic response under frequent earthquakes and mainly behave inelastically under moderate to severe earthquakes. The entire design optimisation procedure can thus be categorized into two phases: “elastic phase” and “inelastic phase”.

2.5.1. Elastic phase: element size optimisation

The performance objective at this stage is to satisfy Immediate Occupancy (IO) criteria under frequent earthquakes in accordance with 50 % probability of exceedance in 50 years (here PGA = 0.1 g as shown in Table 1). The key performance parameter for controlling the structural response of elastic (or near-elastic) systems is considered to be inter-storey drift ratio (IDR). The first phase considers elements sizes as a single design variable, considering that the concrete section size plays a more dominant role in providing lateral stiffness and hence controlling inter-storey drift ratios. The element size optimisation algorithm is briefly summarised as follows:

1. The RC frame is initially designed in accordance with a conventional code-based design method. In this study, Eurocode 8 is used for preliminary designs of the selected frames. The details of cross-section dimensions and reinforcement ratios of the initial design solutions are provided in Appendix A.
2. The designed structure is subjected to a set of spectrum-compatible frequent earthquake records (scaled to PGA = 0.1 g) corresponding to IO performance level. Maximum IDR at each storey ($\Delta_{max,i}$) is obtained as average of the maximum values under the selected earthquakes to capture record-to-record variability, through non-linear time-history analysis, using the following equation (2):

$$\Delta_{max,i} = \frac{\delta_i - \delta_{i-1}}{h_i} \tag{2}$$

where, δ_i and δ_{i-1} are the relative maximum lateral displacement of two adjacent i and i-1 floor levels, respectively; and h_i is storey height at i^{th} floor.

3. When the IDR in a certain storey is higher than the target limit, the specific performance objective is in turn violated, and hence structural capacity should be increased by adding more material. On the other hand, in storeys where IDR is less than the target value, structural materials are not fully utilised. Therefore, the concrete section dimensions (here size of column square cross-sections (D), width (B) and depth (H) of beam rectangular cross-sections) are reduced or increased accordingly as discrete design variables by using the equations (3)-(8):

If $\Delta_{max,i} \leq \Delta_{target,i}$

$$[B_i]_{n+1} = [B_i]_n - \Delta B \tag{3}$$

$$[H_i]_{n+1} = [H_i]_n - \Delta H \tag{4}$$

$$[D_i]_{n+1} = [D_i]_n - \Delta D \tag{5}$$

If $\Delta_{max,i} > \Delta_{target,i}$

$$[B_i]_{n+1} = [B_i]_n + \Delta B \tag{6}$$

$$[H_i]_{n+1} = [H_i]_n + \Delta H \tag{7}$$

$$[D_i]_{n+1} = [D_i]_n + \Delta D \tag{8}$$

where $\Delta_{target,i}$ is the pre-decided target drift value of i^{th} storey corresponding to IO (i.e. 1 %); $[D_i]_n$ represents dimensions of columns of each storey (i denotes i^{th} storey) at n^{th} iteration; $[B_i]_n$ and $[H_i]_n$ are beams widths and heights at i^{th} storey in n^{th} iterative step, respectively; ΔD, ΔB and ΔH denote small dimension step changes in columns, beams widths and beams heights, respectively. Based on practical considerations, the cross-section dimension changes are set at 50 mm. It should be noted that the reinforcement ratio of each beam and column element is initially designed and kept unchanged during the entire element size optimisation when the structure behaves nearly elastically.

4. The coefficient of variation (COV) of inter-storey drifts (calculated as standard deviation of IDRs divided by the average of IDRs across all storeys) is calculated at each iterative step. Steps 2 and 3 are repeated iteratively until the COV is lower than a given value, maximum IDR in each storey is satisfied with target limit at IO level. It should be noticed that since the optimum design solution is also required to sustain gravity loads, section sizes in lower stories are usually larger than the codified minimum value, and hence it is very unlikely to achieve a very uniform inter-storey drift distribution due to practical applications.

2.5.2. Inelastic phase: reinforcement ratios optimisation

Once optimum concrete section sizes are obtained at the end of the elastic design optimisation phase, they are used as the initial design in the second phase of optimisation. At this stage, longitudinal reinforcement ratios are used as primary design variables. This can be justified as steel reinforcement plays a dominant role in controlling inelastic responses beyond the occurrence of first yielding and providing structural ductility. In accordance to ASCE 41-17 [50], multiple performance objectives including Life Safety (LS) and Collapse Prevention (CP) should be satisfied in the plastic phase, under earthquake excitations with different hazard levels (PGA = 0.4 g; 0.65 g) as mentioned in Table 1. Performance parameters at structural (i.e. inter-storey drift) and element (i.e. plastic hinge rotation) levels are simultaneously considered in the optimisation process at both specific performance levels.

The steps for UDD optimisation in the plastic phase are as follows:

1. Optimum structural design obtained at the end of elastic phase is regarded as initial design in the plastic design optimisation phase.
2. Plastic hinge rotations at both ends of beam and column elements are calculated based on plastic curvatures (k^p) and in accordance with "Modified Gauss-Radau" plastic hinge integration method as suggested by [51]:

$$\begin{bmatrix} \theta_I \\ \theta_J \end{bmatrix} = \begin{bmatrix} -k^p|_{x=0} \times l_{pI} \\ k^p|_{x=L} \times l_{pJ} \end{bmatrix} \tag{9}$$

where: θ_I and θ_J are plastic rotations at ends I and J of an element, respectively; $x = 0$ and $x = L$ describe the locations of integration points (both ends of an element); l_{pI} and l_{pJ} are physical length of plastic hinge near ends I and J, respectively; $k^p|_{x=0}$ and $k^p|_{x=L}$ are plastic curvatures at both ends of the element. Average maximum plastic rotations under a set of earthquakes in a certain storey can in turn be obtained for column and beam elements using the equations (10)-(11):

$$\theta_{max,i,C} = \max\left[\theta_{n=1,I}, \theta_{n=1,J}, \theta_{n=2,I}, \theta_{n=2,J} \cdots \theta_{n=N_{col},I}, \theta_{n=N_{col},J}\right] \tag{10}$$

$$\theta_{max,i,B} = \max\left[\theta_{n=1,I}, \theta_{n=1,J}, \theta_{n=2,I}, \theta_{n=2,J} \cdots \theta_{n=N_{beam},I}, \theta_{n=N_{beam},J}\right] \tag{11}$$

where: $\theta_{max,i,C}$ and $\theta_{max,i,B}$ are the peak column plastic hinge rotation and peak beam plastic hinge rotation in i^{th} storey, respectively; N_{col} is total number of columns elements in each storey (i.e. $N_{col} = 4$); N_{beam} is total number of beam elements in each storey (i.e. $N_{beam} = 3$).

3. The performance ratios $PR_{drift,i}$, $PR_{rotation,i,C}$ and $PR_{rotation,i,B}$ are calculated as ratios of deformation demands to corresponding capacity in each storey, column member and beam member, respectively.

$$PR_{drift,i} = \frac{\Delta_{max,i}}{\Delta_{target}} \tag{12}$$

$$PR_{rotation,i,C} = \frac{\theta_{max,i,C}}{\theta_{target,i,C}} \tag{13}$$

$$PR_{rotation,i,B} = \frac{\theta_{max,i,B}}{\theta_{target,i,B}} \tag{14}$$

where: Δ_{target} equals to 2 % at LS level and 4 % at CP level; $\theta_{target,i,C}$ and $\theta_{target,i,B}$ are plastic rotation capacity of column and beam elements, respectively, determined in accordance with ASCE 41-13 [7].

Multi performance levels (here LS and CP) are concurrently considered, and design variables are remodified based on the most critical performance ratio ($PR^{critical}$) chosen as the largest value from the ratios relating to all specific performance levels:

$$PR^{critical}_{drift,i} = \max\left[PR^{K=I}_{drift,i}, PR^{K=II}_{drift,i}, \cdots PR^{K=n}_{drift,i}\right] \tag{15}$$

$$PR^{critical}_{rotation,i,C} = \max\left[PR^{K=I}_{rotation,i,C}, PR^{K=II}_{rotation,i,C}, \cdots PR^{K=n}_{rotation,i,C}\right] \tag{16}$$

$$PR^{critical}_{rotation,i,B} = max\left[PR^{K=I}_{rotation,i,B}, PR^{K=II}_{rotation,i,B}, \cdots PR^{K=n}_{rotation,i,B}\right] \tag{17}$$

where: K = I, II, n denotes pre-decided performance objectives (here I = LS performance level under DBE, II = CP performance level under MCE); $PR^{critical}_{drift,i}$ is the critical drift performance ratio considering drift responses in i^{th} storey level; and $PR^{critical}_{rotation,i,C}$, $PR^{critical}_{rotation,i,B}$ are critical performance ratios considering rotations in columns and beams, respectively.

The proposed method considers plastic hinge rotation as the main performance parameter, while IDR is only accounted in UDD optimisation when the target IDR is violated (i.e.$PR^{critical}_{drift,i} > 1$). To provide more practical design solutions, it is assumed that in each storey, both interior and exterior columns have the same reinforcement ratio. Furthermore, in the selected models, all beam elements in one storey were designed to have similar reinforcement detailing as the span lengths are identical. The longitudinal reinforcement ratios of beams and columns in each storey are modified using the equations (18)-(21):

If $PR^{critical}_{drift,i} > 1$ and $max[\mathrm{PR}^{critical}_{rotation,i,C}, PR^{critical}_{rotation,i,B}]\langle 1$ ::

$$[(\rho_C)_i]_{n+1} = [(\rho_C)_i]_n \times \left(PR^{critical}_{drift,i}\right)^{\beta} \times \left(1 - \left(PR^{critical}_{rotation,i,C}\right)^{(-\beta)}\right) \tag{18}$$

$$[(\rho_B)_i]_{n+1} = [(\rho_B)_i]_n \times \left(PR^{critical}_{drift,i}\right)^{\beta} \times \left(1 - \left(PR^{critical}_{rotation,i,B}\right)^{(-\beta)}\right) \tag{19}$$

In the other conditions:

$$[(\rho_C)_i]_{n+1} = [(\rho_C)_i]_n \times \left(PR^{critical}_{rotation,i,C}\right)^{(\alpha)} \tag{20}$$

$$[(\rho_B)_i]_{n+1} = [(\rho_B)_i]_n \times \left(PR^{critical}_{rotation,i,B}\right)^{(\alpha)} \tag{21}$$

where: $[(\rho_C)_i]_n$ and $[(\rho_B)_i]_n$ represent reinforcement ratios in columns and beam in i^{th} storey at n^{th} iteration, respectively; β is a convergence parameter in the UDD formula which involves both local and global performance parameters, while α is a convergence parameter that controls optimisation speed when only one design parameter is considered. Based on results on the effect of convergence parameters on optimum solutions in the following section, α was considered to be equal to 0.2,

Fig. 1. Geometry and dimensions of beam and column members of 3-, 5-, 10- and 15-storey RC frames (Beams: "height × width"; Columns: "square dimension").

while β was assumed to be half of α.

4. When the modified reinforcement is below the minimum allowable values, the minimum values are used. However, if the reinforcement ratio exceeds the maximum allowable value, the element size (D, B and H) in i^{th} storey at $(n+1)^{th}$ iteration is incrementally increased using the following equations (22)-(25):

If reinforcement ratio in a column reaches the maximum allowable value:

$$[D_i]_{n+1} = [D_i]_n + \Delta D \tag{22}$$

If tension or compression reinforcement ratio in a beam reaches the upper limit:

$$[B_i]_{n+1} = [B_i]_n + \Delta B \tag{23}$$

$$[H_i]_{n+1} = [H_i]_n + \Delta H \tag{24}$$

$$[D_i]_{n+1} = [D_i]_n + \Delta D \tag{25}$$

where: D and ΔD are dimensions of the column cross section and corresponding dimension increment, respectively; B and ΔB are beam widths and corresponding size increment, respectively; H and ΔH are beam height and corresponding size increment, respectively. ΔD, ΔB and ΔH are all taken as 50 mm to provide practical solutions and avoid a sudden increase in structural stiffness.

5. The COV(%) of IDR and plastic hinge rotations in each storey are calculated at both LS and CP performance levels. The UDD algorithm iterates from step 2 until the following conditions are met: (i) the calculated COVs are decreased to an acceptable value (e.g. less than 0.2), (ii) the given performance parameters in each storey are fully satisfied with the target limits corresponding to both LS and CP levels, and their changes remain small at a few subsequent iterations. As discussed before, it is also checked that the final optimum design can sustain the gravity loads.

3. Modelling and assumptions

3.1. Reference reinforced concrete frames

To assess the efficiency of the proposed optimisation framework, four different 3-bay RC frames with 3-, 5-, 10- and 15-storey were selected, with a uniform height of 3 m as shown in Fig. 1. The buildings were considered to represent typical residential buildings in high seismic regions, with importance class I and medium ductility class (DCM). The seismic loads were calculated using the Eurocode 8 design response spectrum for medium seismic regions (peak ground acceleration (PGA) 0.4 g). The dead and live loads for intermediate storeys were taken to be 4.6 kN/m^2 and 2 kN/m^2, while for the roof the dead and live loads were reduced to 4 kN/m^2 and 0.7 kN/m^2, respectively. The frames were assumed to be located on soil type C, and to account for structural nonlinearly a behaviour factor q = 3.9 was considered. The nominal compressive strength of concrete and yielding strength of steel reinforcement were 30 MPa and 500 MPa, respectively. The initial frames satisfied safety, serviceability and durability design criteria of Eurocode 2 and 8 [1,44].

The frames were modelled and analysed using the finite element software OpenSees [48]. "Concrete02" model was utilised to express the material properties of concrete, considering stress–strain relationships of both confined and unconfined concrete by taking into account tension cracking and compressive crushing failure mechanisms [52]. "Steel02" (or Giuffre-Menegotto-Pinto) model was considered to simulate the bilinear stress–strain relationship of reinforcement steel [53]. Beam and column elements were modelled using "distributed-plasticity models", in which the occurrence of nonlinearity is allowed at any location within a specific range of the element (plastic hinge region) instead of concentrated at both ends of an elastic element [54]. The nonlinear behaviour was analysed using "force-based" nonlinear finite element models ("*forceBeamColumn*"). To obtain more accurate structural inelastic responses (i.e. plastic hinge rotations), the "Modified Gauss-Radau" integration method derived from Gauss-Radau quadrature rule was used. Two integration points are located at the two ends of the element, where the bending moment is largest in the absence of member

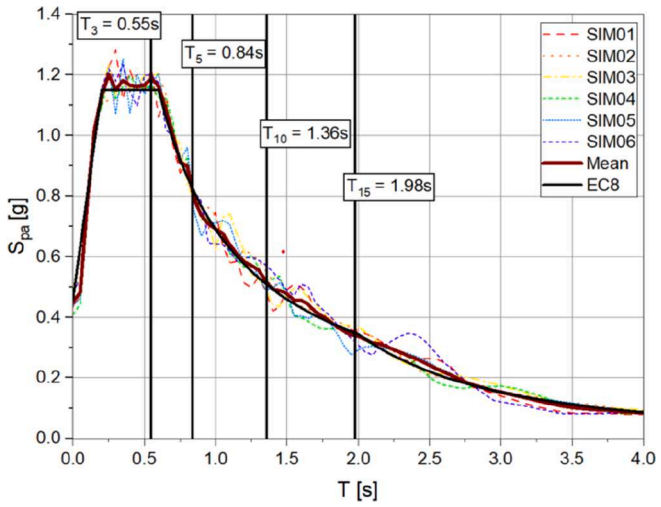

Fig. 2. Eurocode 8 design response spectrum and acceleration spectra of artificial records.

loads, and four integration points along the element length (six integration points in total). The method integrates the deformation over the estimated plastic region using a force-based flexibility formulation, and the element deformation is calculated as the sum of deformations within two plastic hinge regions and one interior section [51]. In this study, the physical length of the plastic hinge region (l_{pl}) was updated in each iterative step using the following formula from Eurocode 8, part 3 [55].

$$l_{pl} = \frac{L_v}{30} + 0.17h + 0.24\frac{d_{bL}f_y(MPa)}{\sqrt{f_c}(MPa)} \tag{26}$$

where d_{bL}, f_y and f_c are mean diameter of tension reinforcement, concrete compressive strength and steel yield strength, respectively. L_v is the shear span at member ends, and h is the depth of the cross-section.

The above formulation indicates that the plastic hinge length depends on the variation of stiffness (cross-section size, diameter of reinforcement) and material properties. It should be noted that these material and element models are extensively used, as they simulate well the nonlinear behaviour of RC structures under seismic and cyclic lateral loads [56,57].

Rayleigh damping with a constant ratio of 5 % was assigned to the first model and any mode whose cumulative mass participation exceeds 95 %. P-Delta effects were also considered for both the design and analyses of the frames. Soil-structure interaction (SSI) effects were not taken into account. To consider the effect of concrete cracking on overall element stiffness, the effective flexural and shear stiffnesses of beam and column elements were taken as half of the gross section stiffness values, as recommended by Eurocode 8.

3.2. Selected earthquake records and code-based design spectrum

In this study, a set of six seismic ground motion records fully compatible with the target spectrum were synthesised using target acceleration spectra compatible time histories (TARSCTHS) [58]. The elastic response spectrum of each of the generated records as well as their mean response spectrum are compared with the Eurocode 8-based elastic design response spectrum in Fig. 2. It can be seen that the mean response spectrum of the artificial records provides a close approximation to the Eurocode 8 design spectrum within a wide range of periods that cover the fundamental periods of the four selected RC frames. Therefore, the selected artificial earthquakes can be considered as suitable representatives of the chosen design spectrum. For different hazards levels, the generated records are simply scaled to reach the target PGA level.

4. Optimum design for the design earthquakes

4.1. Seismic performance assessment

For each referenced frame, the average seismic responses (i.e. IDR and plastic rotations ratios) under all six records are calculated and compared between the optimum solution (named as “optimum design”) and the initial design codified by Eurocode 8 (named as “initial design”).

Fig. 3 compares the height-wise distributions of maximum inter-storey drift ratios (Δ_{max}) for the 3-, 5-, 10- and 15-storey RC frames at IO, LS, CP performance levels. Compared to the initial frames, the frames optimised based on the concept of UDD exhibited more uniform inter-storey drift distribution, and less concentrated maximum inter-storey drifts, while they closely approached the performance targets at each specific seismic hazard level. The optimum designs also reduce global damage, as details will be explained in the following sections.

Figs. 4, 5, 6 and 7 illustrate the height-wise distributions of maximum plastic rotation ratios in columns ($\theta_{max,C}/\theta_{target,C}$) for 3-, 5-, 10- and 15-storey optimum and initial designs. The results represent the average values under the selected six artificial records corresponding to LS and CP performance levels subjected to DBE and MCE records, respectively. It can be seen that the optimum solutions generally experienced less maximum plastic rotation ratios and localised damage concentration. It should be noted that in some cases the optimum designs exhibited larger plastic rotation ratios than their initial design counterparts (e.g. first storey in 3-storey frame, and first three storeys in 15-storey frame). This is because the optimum solutions use smaller column cross sections in these storeys to achieve a more efficient use of material capacity. This leads to higher axial load ratios in these elements, which also affects their rotational capacity.

Tables 4, 5 and 6 present the average maximum responses in terms of inter-storey drift, and plastic rotation in columns and beams, respectively, for optimum and initial designs at different performance levels. The results demonstrate that the proposed optimum design framework reduces maximum inter-storey drift ratios up to 15 %, 36 %, 58 % and 23 % for 3-, 5-, 10- and 15-storey frames, respectively. When structures are subjected to DBE and MCE earthquake records, optimum design solutions also result in significant reductions in maximum plastic rotation ratios in beams and columns up to 13 %, 42 %, 78 % and 20 % for 3-, 5-, 10- and 15-storey frames, respectively. It can be concluded that, compared to the initial designs, the proposed optimisation technique is helpful in improving the structural safety of all the selected frames at IO, LS and CP performance levels by reducing localised damage and preventing soft storey failures. In optimum design solutions, material capacities in most of storeys are fully exploited, which in turn leads to a more uniform performance distribution aligned with the concept of UDD.

As an example, Table 7 presents the details on section dimensions of the 10-storey RC frame for both optimum and initial designs. In the optimum design, the element cross section dimensions were only increased in the top storeys, while the dimensions of most sections were reduced to achieve more efficient material usage. The difference in total volume of concrete used in the beams and columns in the 10-storey frames is found to be 20 %.

In general, the optimum design solutions required considerably lower reinforcement ratios to satisfy the selected performance target. As an example, Table 8 presents the longitudinal steel reinforcement design details of beams and columns of the 5-storey RC frame before and after optimisation. It can be noted that in the optimum design the ratios of columns and beams in several storeys tend to the minimum allowable limits in Eurocode 8 so that material can be more efficiently used. The dimensions of such sections cannot be reduced otherwise the IO design targets will be violated. The difference in total weight of reinforcement steels used in the beams and columns in the 5-storey frames is found to be 43 %. More information about cross-section dimensions and longitudinal reinforcement ratio of initial and optimum design solutions for

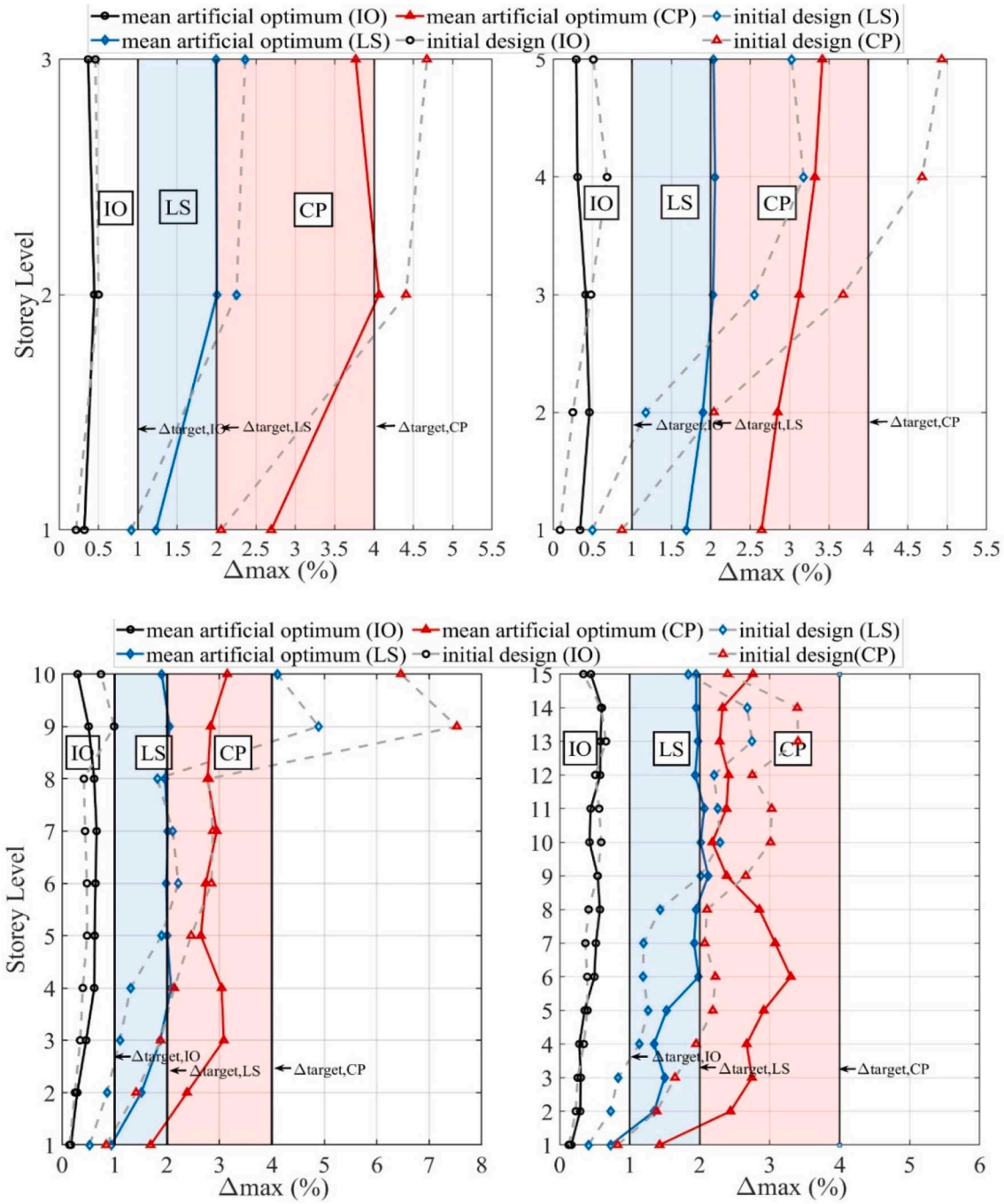

Fig. 3. Height-wise distribution of Δ_{max} for optimum and initial design solutions for 3-, 5-, 10- and 15-storey frames, average results under six artificial records at IO, LS, CP performance levels.

3-, 5-, 10- and 15-storey RC frames are presented in the tables in Appendix A and B.

4.2. Global damage index

Previous studies indicated that maximum inter-storey drift ratios may not always accurately predict damage state of a structure, especially when the structure dissipates a large amount of earthquake input energy through large plastic deformations [59,60]. To investigate the efficiency of the proposed optimisation method on reducing overall structural damage during an earthquake event, this study quantifies the damage by using the damage index which is evaluated as a function of displacement ductility and dissipated energy. To achieve this, the structural damage index in the i^{th} storey (D_i) is first estimated, using the "demand versus capacity" concept as suggested by [61]:

$$D_i = \left(\frac{\delta_c - \delta_t}{\delta_u - \delta_t}\right)^b \tag{27}$$

where δ_c, δ_t and δ_u are the calculated, threshold and ultimate values of specific damage parameter, respectively. Constant parameter b is determined based on experimental data, which is suggested as 1.5 for reinforced concrete frames [62].

In this study, the displacement-based ductility ratio (μ) is considered as the damage parameter to evaluate the structural ability to deform within the inelastic range before failure. The maximum ductility ratio

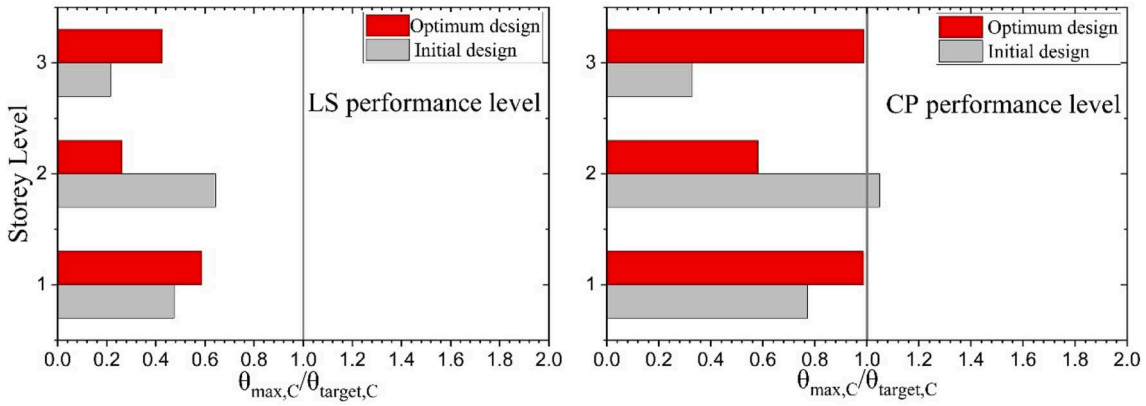

Fig. 4. Height-wise distribution of $\theta_{max,C}$ to $\theta_{target,C}$ ratios for optimum and initial design 3-storey frame, average results under six artificial records at LS and CP performance levels.

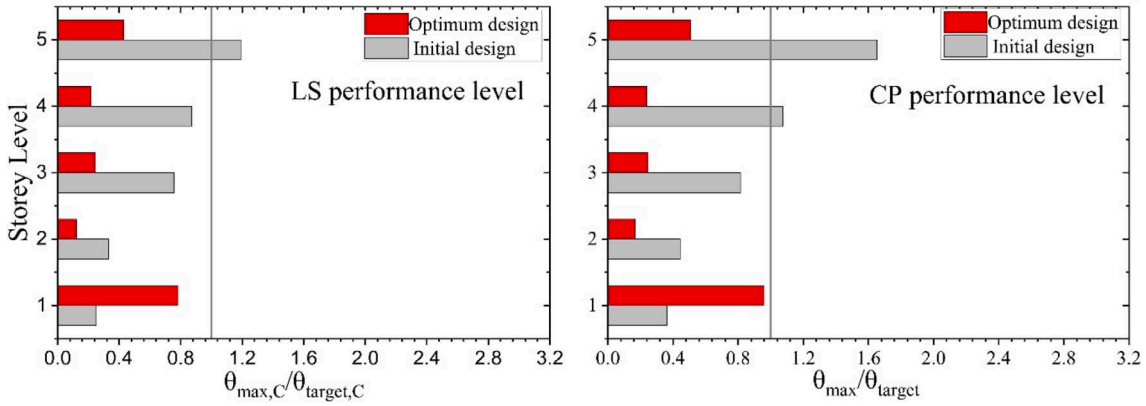

Fig. 5. Height-wise distribution of $\theta_{max,C}$ to $\theta_{target,C}$ ratios for optimum and initial design 5-storey frame, average results under six artificial records at LS and CP performance levels.

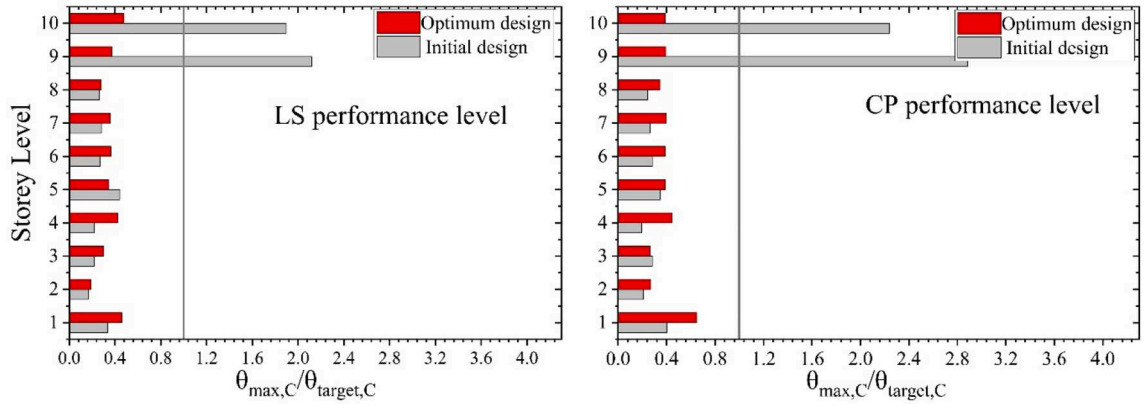

Fig. 6. Height-wise distribution of $\theta_{max,C}$ to $\theta_{target,C}$ ratios for optimum and initial design 10-storey frame, average results under six artificial records at LS and CP performance levels.

(μ_{max}) can be obtained using the equation (28):

$$\mu_{max} = \frac{\Delta_{max,i}}{\Delta_{yield,i}} \tag{28}$$

And the corresponding ultimate ductility ($\mu_{ultimate}$) is calculated as:

$$\mu_{ultimate} = \frac{\Delta_{ultimate,i}}{\Delta_{yield,i}} \tag{29}$$

where $\Delta_{max,i}$, $\Delta_{yield,i}$ and $\Delta_{ultimate,i}$ represent peak inter-storey drift, yielding drift and ultimate drift capacity in i^{th} storey, respectively. $\Delta_{yield,i}$ can be estimated through pushover analysis by applying a monotonically increasing lateral load and adopting a bilinear representation of the capacity diagram based on equal energy principle as suggested by ASCE 41–13 [7]. In this study, $\Delta_{ultimate,i}$ is assumed to be the target limiting value at CP performance level in accordance with ASCE 41–06 [47], and the value is for structural failure is assumed to occur. Using the defined ductility parameters, Equation (28) can be written as follows to calculate the storey damage index corresponding to i^{th} storey (D_i):

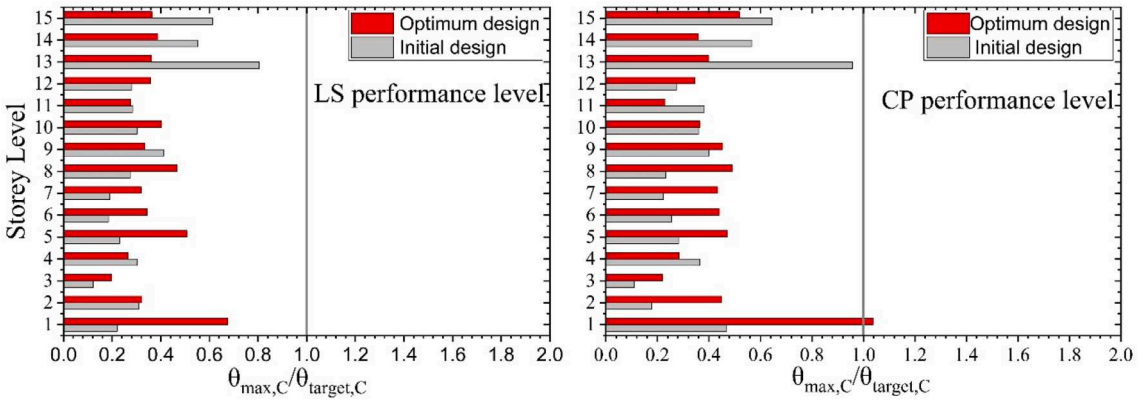

Fig. 7. Height-wise distribution of $\theta_{max,C}$ to $\theta_{target,C}$ ratios for optimum and initial design 15-storey frame, average results under six artificial records at LS and CP performance levels.

Table 4
Maximum Δ_{max} (%) of 3-, 5-, 10- and 15-storey frame with optimal and initial design solutions.

Performance Level	Immediate Occupancy			Life Safety			Collapse Prevention		
RC frames	Optimum	Initial	Gain	Optimum	Initial	Gain	Optimum	Initial	Gain
3-storey	0.45	0.50	10.7 %	2.00	2.36	15.4 %	4.04	4.68	13.2 %
5-storey	0.46	0.68	32.8 %	2.04	3.18	35.6 %	3.40	4.96	31.2 %
10-storey	0.65	1.01	35.3 %	2.08	4.88	57.5 %	3.16	7.48	57.9 %
15-storey	0.60	0.66	9.0 %	2.12	2.74	22.9 %	3.28	3.30	3.1 %

$$D_i = \left(\frac{\Delta_{max,i} - \Delta_{yield,i}}{\Delta_{ultimate,i} - \Delta_{yield,i}}\right)^b \tag{30}$$

This damage index formula assumes that the largest damage in each storey is expected to happen where inter-storey drift ratio at i^{th} level reaches the maximum value during the earthquake.

Subsequently, the global damage index D_g is defined as weighted average of damage index D_i at individual storey levels:

$$D_g = \frac{\sum_{i=1}^{N} D_i w_i}{\sum_{i=1}^{N} w_i} \tag{31}$$

In the above equation, N represents the total number of storeys. w_i is the weight factor for i^{th} storey represented by dissipated energy. Here it is assumed that the amount of energy dissipation corresponding in each storey is proportional to its damage index, D_i, as suggest by previous studies [63,38]. The global damage index D_g ranges from 0 (undamaged) to 1 (completely damaged).

Fig. 8 shows the mean global damage indices of 3, 5, 10 and 15-storey RC optimum design frames compared to their code-based design counterparts under the six selected earthquakes. The results indicate that the UDD optimisation led to less overall damage at both LS and CP performance levels. It is shown that, compared to the initial frames, the optimum design solutions experience less damage up to 64 %, 51 %, 88 % and 52 % for 3, 5, 10 and 15-storey frames, respectively. This is because the proposed optimisation methodology significantly reduces maximum inter-storey drift ratios and prevents "soft storey" failures in the storeys where the response violates the drift limits. Indeed, the drift profiles of all optimum frames tend to be close to the target limits at all specific performance levels in most storeys. Although this cannot be completely achieved due to the influence of axial loads on columns in lower storeys, structural materials at most storey levels are efficiently utilised, which results in a better seismic performance and hence a lower global damage index.

5. Sensitivity analysis

5.1. Effect of convergence parameter

In a nonlinear system, previous studies indicate that changes in the design variables during the iterative process should be made gradually to avoid divergence [64,34,38]. In the proposed UDD optimisation method, the convergence speed is governed by the value of convergence parameter α. A small value of α increases the chance of convergence, but at the expense of increasing computational costs, whilst a larger α reduces computational cost, but may generate significant fluctuations and divergence. This highlights the importance of selecting a suitable value of convergence parameter by considering a balance between computational efficiency and convergence. Figs. 9 and 10 show the variation of maximum inter-storey drift ratios (Δ_{max}) and maximum plastic rotation

Table 5
Maximum Plastic Rotations Demand to Capacity Ratios in Columns of 3-, 5-, 10- and 15-storey frame with optimum and initial design solutions.

Performance Level	Life Safety			Collapse Prevention		
RC frames	Optimum	Initial	Gain	Optimum	Initial	Gain
3-storey	0.59	0.64	8.6 %	0.99	1.05	5.8 %
5-storey	0.78	1.19	34.4 %	0.96	1.65	42.0 %
10-storey	0.46	2.12	78.2 %	0.66	2.89	77.2 %
15-storey	0.68	0.80	16.0 %	1.04	0.96	−8.4 %

Table 6
Maximum Plastic Rotations Demand to Capacity Ratios in Beams of 3-, 5-, 10- and 15-storey frame with optimum and initial design solutions.

Performance Level	Life Safety			Collapse Prevention		
RC frames	Optimum	Initial	Gain	Optimum	Initial	Gain
3-storey	0.80	0.90	11.3 %	0.87	0.99	12.6 %
5-storey	0.68	1.04	34.9 %	0.64	0.90	29.3 %
10-storey	0.54	1.10	50.9 %	0.40	1.05	61.7 %
15-storey	0.52	0.66	20.4 %	0.42	0.44	4.8 %

Table 7
Initial and Optimum Member Sizes (unit: mm) of 10-storey RC frame.

Element	Storey No.	Dimension (Initial)	Dimension (Optimum)	Element	Storey No.	Width (Initial)	Depth (Initial)	Width (Optimum)	Depth (Optimum)
Column	10	300	350	*Beam*	10	300	300	350	300
	9	300	350		9	300	300	350	300
	8	400	350		8	400	350	300	300
	7	400	350		7	400	350	350	300
	6	400	350		6	400	350	350	300
	5	400	350		5	400	350	350	300
	4	450	350		4	450	400	350	300
	3	450	400		3	450	400	400	350
	2	500	450		2	500	450	450	400
	1	500	450		1	500	450	450	400
Total Volume		Initial 43.95 (m^3)						Optimum 35.37 (m^3)	

Table 8
Initial and Optimum Component Reinforcement Ratios (in %) of 5-storey RC frame.

Storey No.	Element	Rein. (Initial)	Rein. (optimum)	Element	Top rein. (Initial)	Bottom rein. (Initial)	Top rein. (optimum)	Bottom rein. (Optimum)
5	*Column*	2.68 %	2.13 %	*Beam*	1.12 %	0.67 %	0.72 %	0.43 %
4		2.68 %	1.01 %		1.12 %	0.67 %	0.35 %	0.35 %
3		1.97 %	1.00 %		0.96 %	0.57 %	0.33 %	0.33 %
2		2.36 %	1.00 %		0.86 %	0.57 %	0.33 %	0.33 %
1		2.01 %	1.02 %		0.36 %	0.27 %	0.33 %	0.33 %
Total Weight		Initial 2480.6 (kg)				Optimum 1428.7 (kg)		

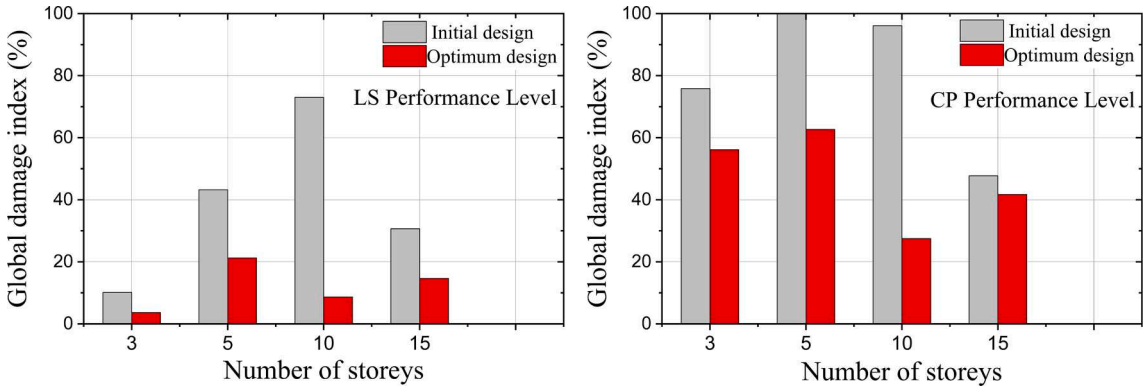

Fig. 8. Global damage index for 3, 5, 10 and 15-storeyy RC frames at LS and CP performance levels, average results under six artificial earthquakes.

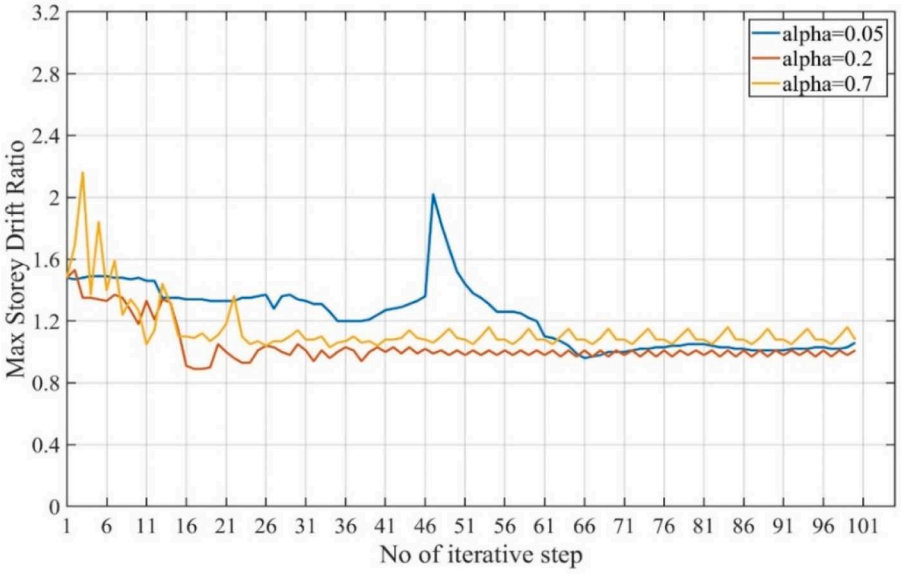

Fig. 9. Maximum Δ_{max} as iterations processed of 5-storey RC frame under, SIM01.

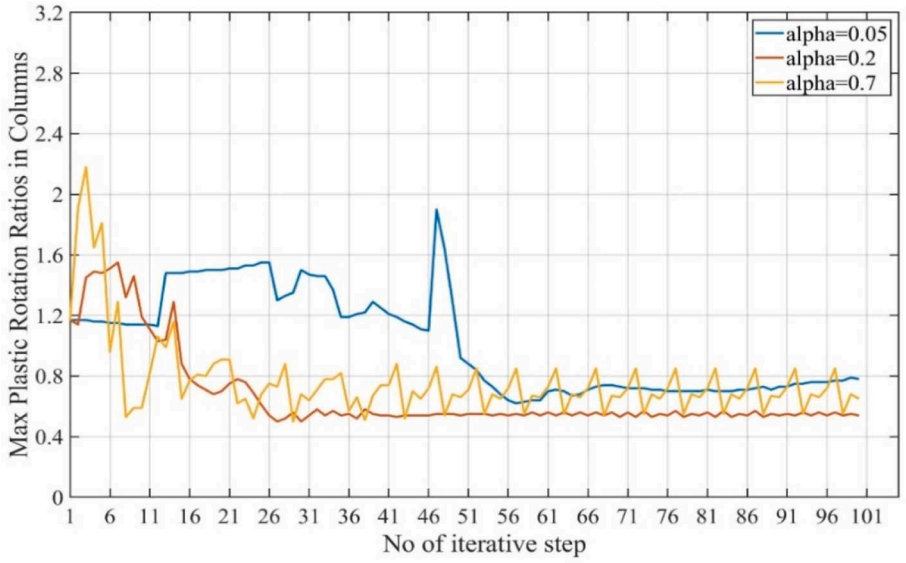

Fig. 10. Maximum $\theta_{max,C}$ as iterations processed of 5-storey RC frame under, SIM01.

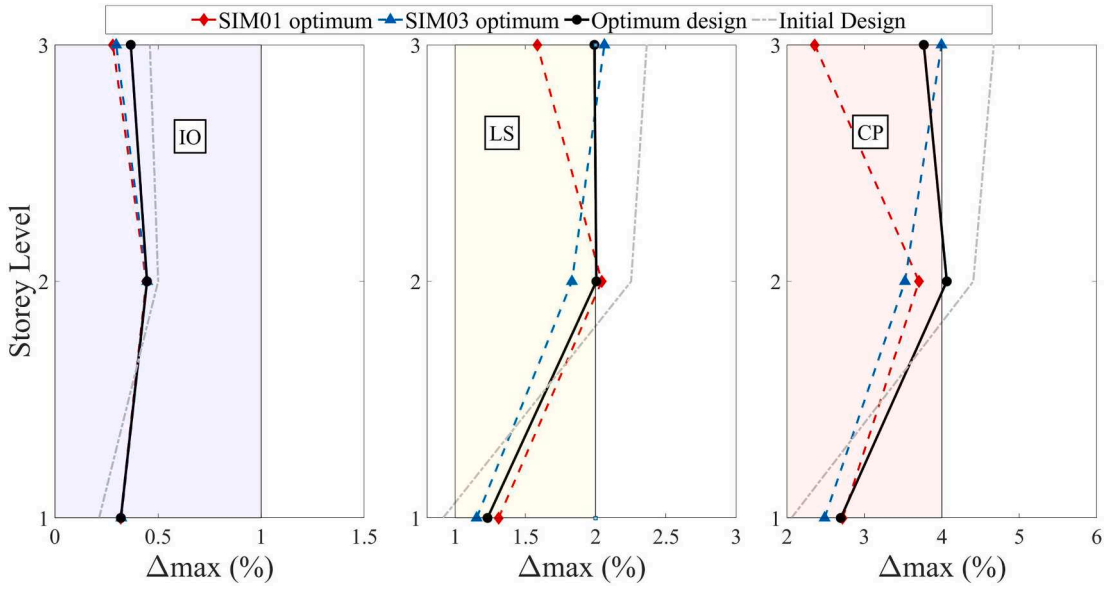

Fig. 11. Efficiency of the selected design approach in terms of average height-wise distribution of Δ_{max} under six artificial earthquakes at IO, LS and CP levels, 3-storey frame.

ratios ($\theta_{max,C}$) of the 5-storey frame versus the iterative steps, for α values equal to 0.005, 0.02 and 0.07, respectively. The results are shown for a single spectrum-compatible artificial earthquake (SIM01) and corresponding to DBE level, but a similar trend was observed for the other earthquake records. It should be noted that the sensitivity analysis started with the optimum solution obtained at the end of the elastic design optimisation.

The results show that the convergence speed is very slow when the convergence parameter α is 0.05. On the other hand, using α equals to 0.7 leads to divergence, which is especially evident in the case of maximum plastic rotations. The α with value of 0.2 provided steady convergence without any major fluctuations, and the final design was practically obtained in less than 40 steps.

It should be noted that Hajirasouliha et al. [33] also suggested using convergence values between 0.1 and 0.2 for single level performance-based optimisation of RC frames. In another study, Nabid et al. [63] demonstrated that reasonable convergent solutions of RC frames with friction dampers can be obtained when the convergence parameter ranges from 0.2 to 0.5. Therefore, the convergence parameter α equal to 0.2 was used for the optimisation in the plastic phase in this study.

5.2. *Effect of earthquake record variability on various design approaches*

Earthquakes are random excitations in nature and their frequency contents and amplitudes in future events cannot be accurately predicted. Consequently, the optimum design solution may be affected by uncertainty associated with different characteristics of the design earthquakes and may change due to the variability of the earthquakes. This section investigates how the uncertainty in the selection of earthquake records affects the design optimisation. Three alternative design approaches are examined: (i), Initial design obtained by following Eurocode 8 regulations (named as “Initial design” in previous sections); (ii), Optimum solution obtained based on the average responses under six chosen earthquake records (named as “Optimum design” in previous sections), (iii), Optimum solutions obtained based on a randomly selected single spectrum-compatible earthquake record, here the optimisation is

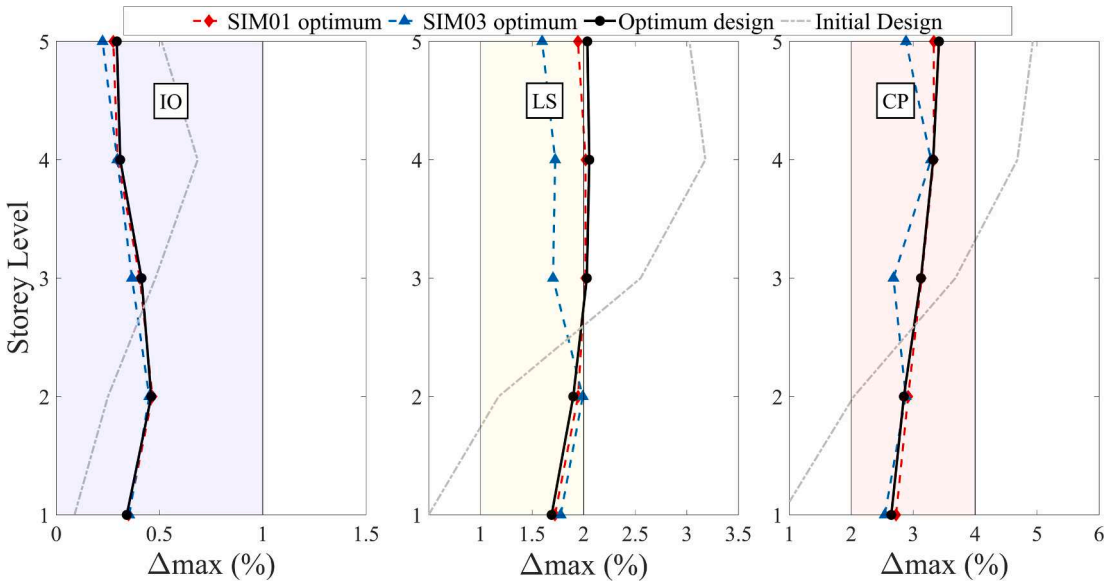

Fig. 12. Efficiency of the selected design approach in terms of average height-wise distribution of Δ_{max} under six artificial earthquakes at IO, LS and CP levels, 5-storey frame.

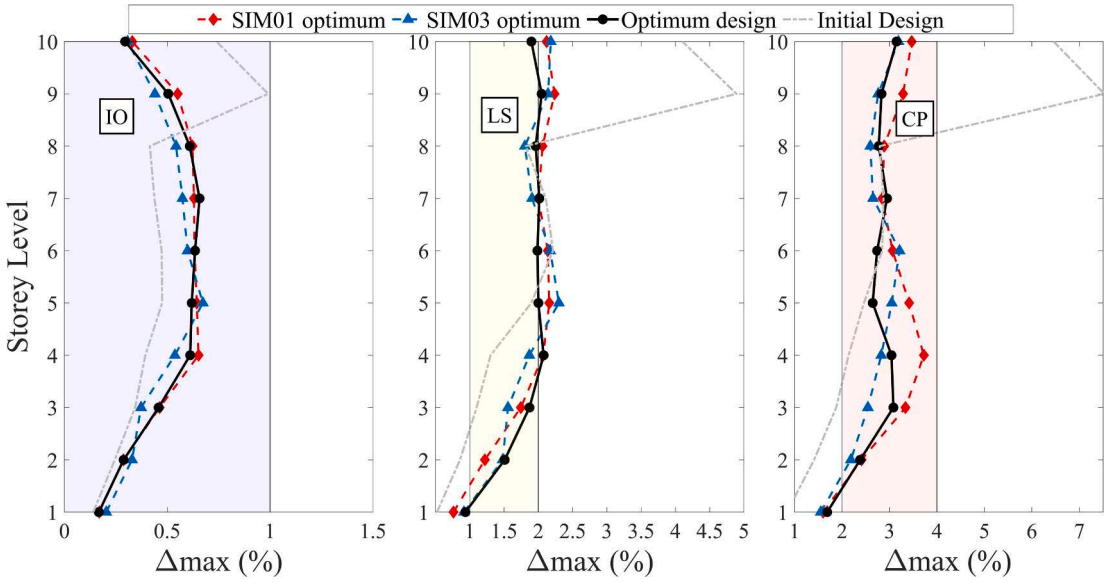

Fig. 13. Efficiency of the selected design approach in terms of average height-wise distribution of Δ_{max} under six artificial earthquakes at IO, LS and CP levels, 10-storey frame.

processed individually under SIM01 and SIM03, respectively (named as "SIM01 optimum" and "SIM03 optimum"). In the third alterative design approaches, the same multi-level optimisation methodology was applied but under a single chosen earthquake record. Nonetheless, for comparison purposes, the performance of the three design approaches is assessed using all six spectrum-compatible artificial earthquakes.

5.2.1. Structural performance of three design approaches

Figs. 11-14 show the effect of earthquake record variability on height-wise distributions of inter-storey drifts at IO, LS and CP performance level for all the reference frames. Figs. 15 and 16 compare, respectively, the maximum plastic rotation ratio and global damage index of 3-, 5-, 10- and 15-storey RC frames designed based on different approaches. It should be noted that the result presented in Fig. 15 is the maximum plastic rotation ratio among all the columns in each of the selected frames. The errors bars in each histogram indicate the corresponding standard deviations of responses under the six artificial earthquake records.

These results demonstrate that, for low to medium-rise buildings (i.e. 3- and 5-storey), the use of single earthquake record (SIM01 or SIM03) can lead to sufficiently accurate seismic responses. In these cases, compared to the code-based initial design, both SIM01 and SIM03 optimum frames exhibited more uniform drift distribution, and satisfied the target PBD limits at all storey levels whilst reducing the local (i.e. maximum plastic rotations) and global damage indexes significantly.

For high-rise buildings (i.e. 10- and 15-storey), the frames designed under both single earthquake records (i.e. SIM01 and SIM03) exhibited discrepancies in the values of Δ_{max} compared to the target limits specified in PBD at LS level (>10 % difference). These frames also experienced larger plastic rotation ratios (up to 59 %) and global damage indexes (up to 36 %) than the corresponding optimum design solutions. These differences are especially evident in the case of the 15-storey

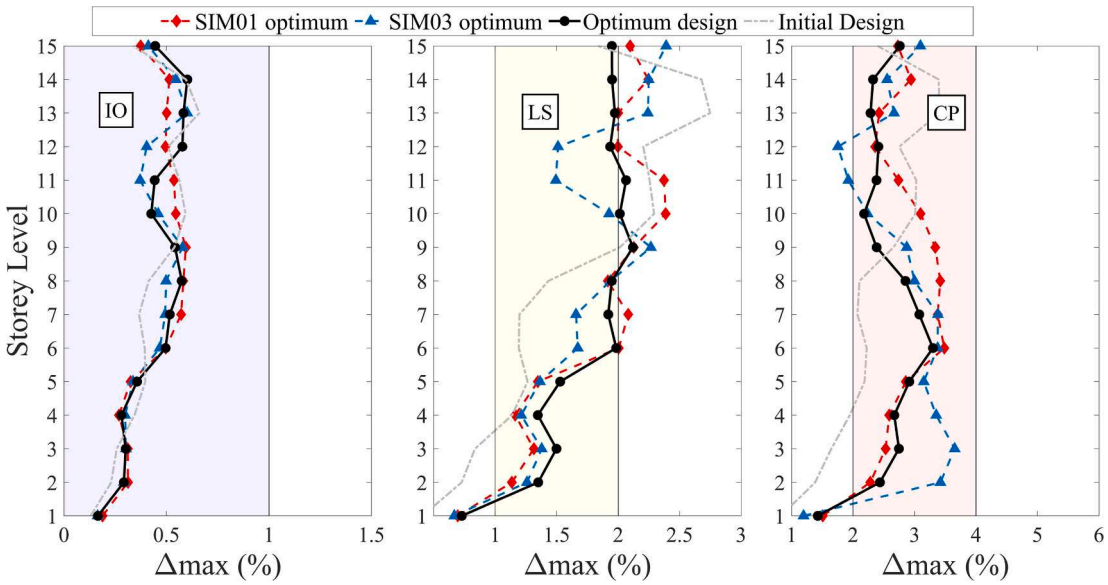

Fig. 14. Efficiency of the selected design approach in terms of average height-wise distribution of Δ_{max} under six artificial earthquakes at IO, LS and CP levels, 15-storey frame.

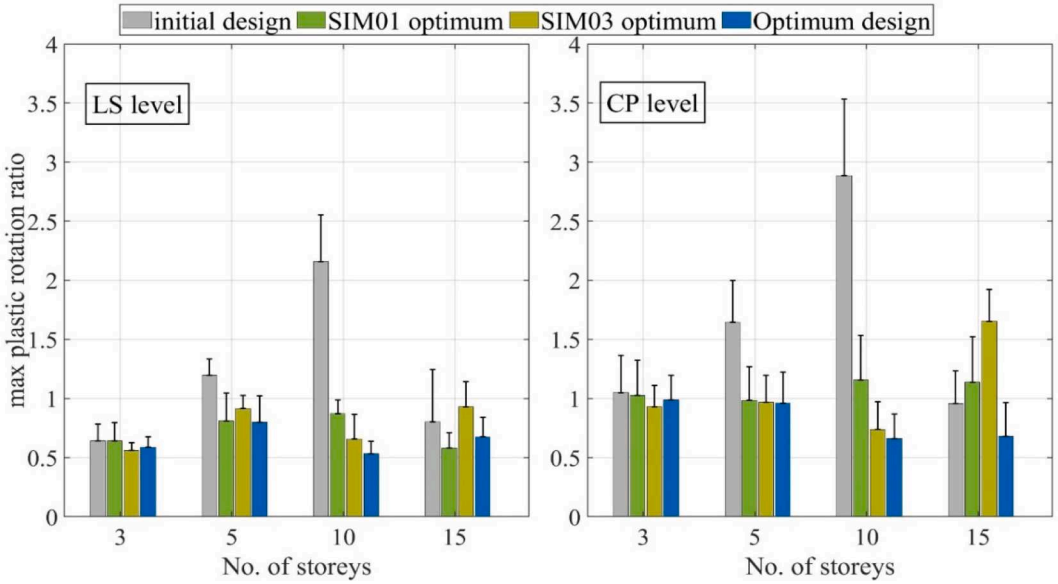

Fig. 15. Max $\theta_{max,C}/\theta_{target,C}$ of 3-, 5-, 10- and 15-storey frame, average results (plus standard deviation) under six selected artificial records at LS and CP levels.

frame at CP performance level. These results can be justified since higher mode effects in tall buildings are generally more prominent and may lead to discrepancies in structural performance when earthquakes with different characteristics are considered.

5.2.2. Material usage of three design approaches

In this section, the effects of earthquake record variability are investigated in terms of the total material usage. The total concrete volume (m^3) and total reinforcement steel weights (kg) required for 3-, 5-, 10-, and 15-storey optimum designs are compared in Table 9, for the different optimisation approaches. It can be seen that, most of the optimum design solutions required less structural materials compared to their code-based initial design counterparts. Furthermore, for the optimisations under single earthquake, the random selection of earthquake record could clearly affect the total materials usage for all the selected RC frames. The results indicate that in the case of low to medium-rise buildings, the optimum solution under a set of earthquakes generally leads to less total material usage, compared to the case that only one input record is used. This is in agreement with the previous observations that by adopting the average response from a chosen set of earthquakes records, the effects of different characteristics of the input design earthquake (i.e. frequency content, amplitude) on the performance assessment can be reduced, and overall, a more reliable design solution is obtained [33].

It should be noted that previous studies demonstrated that design optimisation using a single earthquake record can lead to an acceptable design for steel frames with nonlinear viscous dampers especially in the case of low-to-medium rise buildings [38]. However, this study shows that the design optimisation of RC frames based on a randomly selected single earthquake (e.g. SIM01 or SIM03) may lead to less economic solutions. This is because optimisation of RC frame systems is more complex, since, to achieve practical design solutions, it has to deal with discrete optimisation of section sizes and limits in reinforcement ratios. As a result, the solutions are sensitive to the characteristics of input

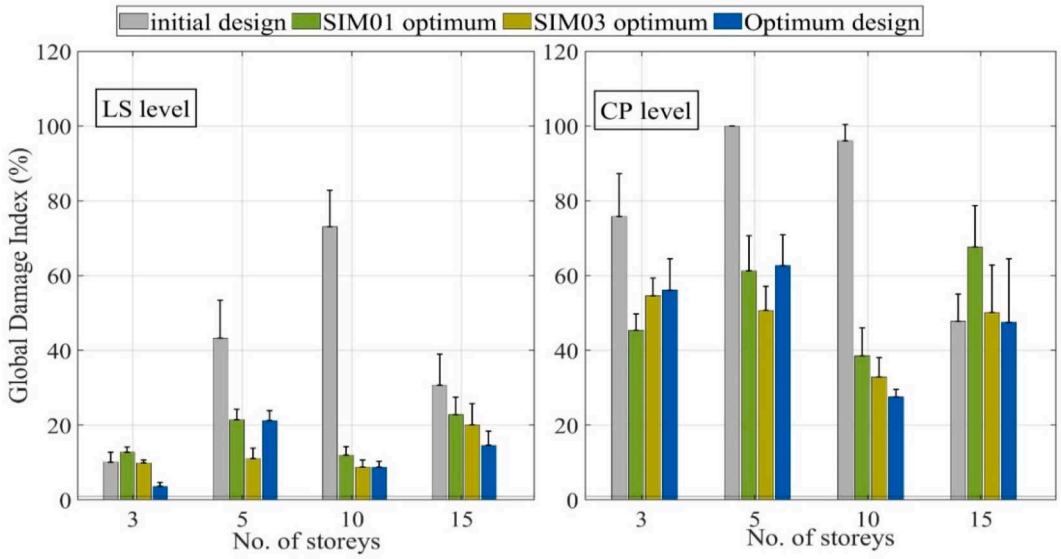

Fig. 16. Global Damage index (%) of 3-, 5-, 10- and 15-storey frame, average results (plus standard deviation) under six selected artificial records at LS and CP levels.

Table 9
Total material usage for four alternative design solutions.

	Total Concrete Volume (m^3)				Total Reinforcement steel weight (kg)			
Design Alternative	Initial design	Optimum design	SIM01 optimum	SIM03 optimum	Initial design	Optimum design	SIM01 optimum	SIM03 optimum
3-Storey	9.66	9.72	10.11	10.11	1318.8	1373.7	1664.2	1397.3
5-Storey	18.30	19.38	19.38	19.77	2480.6	1428.7	1475.8	2464.9
10-Storey	43.95	35.14	35.37	40.01	5809.0	3697.3	3438.3	3297.0
15-Storey	72.40	58.56	58.96	61.68	10063.7	6413.4	5392.9	6264.3

Table A1
Cross-section design details of Beams, 3-storey frames.

Storey Level	Height × Width (cm × cm)	Reinforcement Ratio, top (%)	Reinforcement Ratio, bottom (%)
1	40 × 35	0.67	0.43
2	30 × 30	1.10	0.45
3	30 × 30	1.10	0.45

earthquake records, and hence to obtain reliable design solutions for a specific design spectrum, the average performance under a set of spectrum-compatible records is necessary for the optimisation process.

While the presented results are based on the models and assumptions considered in this study, the proposed multi-level optimisation framework is general, and can be adopted for any design based on other seismic design codes and performance criteria used in common practice.

6. Summary and conclusions

In this study, a multi-level performance-based optimisation framework using the concept of Unform Damage Distribution is proposed to minimise structural damage in multi-storey reinforced concrete frames under earthquake events, while minimising material usage. The key performance parameters, including plastic hinge rotations at the element level and inter-storey drift ratios at the structural level, are simultaneously considered in the optimisation procedure. A novel approach is proposed to optimise both the cross-sectional dimensions of elements and steel reinforcement ratios at elastic and plastic phases, respectively, by satisfying multiple performance-based design criteria and practical design constraints. The efficiency of the proposed method was demonstrated by optimising the design of 3-, 5-, 10- and 15-storey RC frames under a set of spectrum-compatible design earthquake records. From the results presented in this study, the following conclusions can be drawn:

Table A2
Cross-section design details of Columns, 3-storey frames.

Storey Level	Height × Width (cm × cm)	Reinforcement Ratio (%)
1	40 × 40	2.36
2	35 × 35	1.97
3	35 × 35	1.97

Table A3
Cross-section design details of Beams, 5-storey frames.

Storey Level	Height × Width (cm × cm)	Reinforcement Ratio, top (%)	Reinforcement Ratio, bottom (%)
1	50 × 45	0.36	0.27
2	40 × 35	0.86	0.57
3	35 × 30	0.96	0.57
4	30 × 30	1.12	0.67
5	30 × 30	1.12	0.67

Table A4
Cross-section design details of Columns, 5-storey frames.

Storey Level	Height × Width (cm × cm)	Reinforcement Ratio (%)
1	50 × 50	2.01
2	40 × 40	2.36
3	35 × 35	1.97
4	30 × 30	2.68
5	30 × 30	2.68

Table A5
Cross-section details of Beams, 10-storey frames.

Storey Level	Height × Width (cm × cm)	Reinforcement Ratio, top (%)	Reinforcement Ratio, bottom (%)
1	50 × 45	0.70	0.42
2	50 × 45	0.70	0.42
3	45 × 40	0.87	0.45
4	45 × 40	0.87	0.45
5	40 × 35	0.86	0.57
6	40 × 35	0.86	0.57
7	40 × 35	0.86	0.57
8	40 × 35	0.86	0.57
9	30 × 30	1.12	0.45
10	30 × 30	1.12	0.45

Table A6
Cross-section design details of Columns 10-storey frames.

Storey Level	Height × Width (cm × cm)	Reinforcement Ratio (%)
1	50 × 50	2.01
2	50 × 50	2.01
3	45 × 45	1.86
4	45 × 45	1.86
5	40 × 40	2.36
6	40 × 40	2.36
7	40 × 40	2.36
8	40 × 40	2.36
9	30 × 30	1.79
10	30 × 30	1.79

Table A7
Cross-section design details of Beams, 15-storey frames.

Storey Level	Height × Width (cm × cm)	Reinforcement Ratio, top (%)	Reinforcement Ratio, bottom (%)
1	50 × 50	0.75	0.50
2	50 × 50	0.75	0.50
3	50 × 50	0.75	0.50
4	45 × 40	1.05	0.70
5	45 × 40	1.05	0.70
6	45 × 40	1.05	0.70
7	45 × 40	1.05	0.70
8	40 × 35	1.12	0.67
9	40 × 35	1.12	0.67
10	40 × 35	1.12	0.67
11	40 × 35	1.12	0.67
12	40 × 35	1.12	0.67
13	35 × 30	1.15	0.77
14	35 × 30	1.15	0.77
15	35 × 30	1.15	0.77

Table A8
Cross-section design details of Columns, 15-storey frames.

Storey Level	Height × Width (cm × cm)	Reinforcement Ratio (%)
1	55 × 55	1.66
2	55 × 55	1.66
3	55 × 55	1.66
4	45 × 45	1.86
5	45 × 45	1.86
6	45 × 45	1.86
7	45 × 45	1.86
8	45 × 45	1.86
9	40 × 40	2.36
10	40 × 40	2.36
11	40 × 40	2.36
12	40 × 40	2.36
13	35 × 35	1.97
14	35 × 35	1.97
15	35 × 35	1.97

Table B1
Cross-section design details of Beams, 3-storey frames.

Storey Level	Height × Width (cm × cm)	Reinforcement Ratio, top (%)	Reinforcement Ratio, bottom (%)
1	30 × 30	0.33	0.33
2	40 × 35	0.79	0.33
3	30 × 30	1.21	0.49

Table B2
Cross-section design details of Columns, 3-storey frames.

Storey Level	Height × Width (cm × cm)	Reinforcement Ratio (%)
1	40 × 40	3.42
2	40 × 40	1.10
3	30 × 30	3.07

- The proposed multi-level optimisation framework can effectively control the key local and global structural performance parameters to satisfy multiple performance objectives (i.e. IO, LS and CP) under different earthquake intensity levels ranging from frequent to very rare earthquakes. Compared to the initial cade-based design frames, the optimum solutions exhibited lower maximum inter-storey drift ratios and maximum plastic rotation ratios by 58.3 % and 77.5 %, respectively. The optimum structures also, in general, experienced more uniform height-wise distributions of inter-storey drift ratios and plastic rotation ratios, hence preventing local damage.
- In general, the optimum design solutions required considerably less total structural materials by utilising more efficient cross-section sizes and reinforcement ratios. This was particularly evident in the case of 10- and 15- storey frames, where both concrete volumes and total reinforcement weights were reduced by around 20 % and 36 %, respectively. For the 3-storey, the required structural materials were slightly increased (up to 4 %) to satisfy the prescribed performance targets corresponding to multiple hazard levels.
- The magnitudes of global damage index were calculated separately when LS and CP performance levels were considered. The results showed that the 3-, 5-, 10- and 15-storey optimum frames exhibited up to 64 %, 51 %, 88 % and 52 % less global damage index compared to the code-based solutions, respectively.
- The effect of different convergence parameters (α) on the efficiency and computational speed leading to the optimum solution was investigated. It is shown that by using the convergence parameter ($\alpha = 0.2$), the optimum answer is generally achieved in less than 40 steps. This highlights the computational efficiency of the proposed method compared to other optimisation techniques such as GA.
- The effect of earthquake record variability on the optimum design was investigated in terms of both seismic performance and total material usage. It is shown that the design approach based on the proposed optimisation methodology using a single spectrum-compatible earthquake may result in less economic designs and less satisfactory seismic performances especially in the case of tall-buildings. Therefore, to obtain the most robust and economic

Table B3
Cross-section design details of Beams, 5-storey frames.

Storey Level	Height × Width (cm × cm)	Reinforcement Ratio, top (%)	Reinforcement Ratio, bottom (%)
1	30 × 30	0.33	0.33
2	45 × 40	0.33	0.33
3	40 × 35	0.33	0.33
4	40 × 35	0.35	0.35
5	30 × 30	0.73	0.44

Table B4
Cross-section design details of Columns, 5-storey frames.

Storey Level	Height × Width (cm × cm)	Reinforcement Ratio (%)
1	45 × 45	1.02
2	45 × 45	1.00
3	40 × 40	1.00
4	40 × 40	1.01
5	30 × 30	2.13

Table B5
Cross-section details of Beams, 10-storey frames.

Storey Level	Height × Width (cm × cm)	Reinforcement Ratio, top (%)	Reinforcement Ratio, bottom (%)
1	45 × 40	0.32 %	0.32 %
2	45 × 40	0.32 %	0.32 %
3	40 × 35	0.32 %	0.32 %
4	35 × 30	1.22 %	0.62 %
5	35 × 30	1.46 %	0.97 %
6	35 × 30	0.97 %	0.65 %
7	35 × 30	1.01 %	0.67 %
8	30 × 30	1.17 %	0.78 %
9	35 × 30	0.98 %	0.47 %
10	35 × 30	0.35 %	0.35 %

Table B6
Cross-section design details of Columns 10-storey frames.

Storey Level	Height × Width (cm × cm)	Reinforcement Ratio (%)
1	45 × 45	1.00 %
2	45 × 45	1.00 %
3	40 × 40	1.00 %
4	35 × 35	1.87 %
5	35 × 35	2.44 %
6	35 × 35	1.89 %
7	35 × 35	1.53 %
8	35 × 35	1.45 %
9	35 × 35	1.53 %
10	35 × 35	1.42 %

design solution, it is recommended to use optimisation based on the average response of a set of spectrum-compatible records.

CRediT authorship contribution statement

Geyu Dong: Writing – original draft, Methodology, Software, Formal analysis, Investigation, Data curation, Visualization. **Iman Hajirasouliha:** Writing – review & editing, Conceptualization, Methodology, Validation, Supervision. **Kypros Pilakoutas:** Writing – review & editing, Methodology, Validation, Supervision. **Payam Asadi:** Writing – review & editing, Validation.

Table B7
Cross-section design details of Beams, 15-storey frames.

Storey Level	Height × Width (cm × cm)	Reinforcement Ratio, top (%)	Reinforcement Ratio, bottom (%)
1	45 × 40	0.60 %	0.40 %
2	45 × 40	0.60 %	0.40 %
3	45 × 40	0.60 %	0.40 %
4	45 × 40	0.80 %	0.53 %
5	40 × 35	0.80 %	0.53 %
6	35 × 30	0.81 %	0.55 %
7	40 × 35	1.09 %	0.73 %
8	35 × 30	0.30 %	0.30 %
9	40 × 35	1.30 %	0.78 %
10	40 × 35	0.60 %	0.38 %
11	40 × 35	0.81 %	0.49 %
12	35 × 30	1.10 %	0.66 %
13	35 × 30	1.25 %	0.84 %
14	30 × 30	1.48 %	0.99 %
15	30 × 30	0.61 %	0.40 %

Table B8
Cross-section design details of Columns, 15-storey frames.

Storey Level	Height × Width (cm × cm)	Reinforcement Ratio (%)
1	45 × 45	1.80 %
2	45 × 45	1.00 %
3	45 × 45	1.00 %
4	45 × 45	1.00 %
5	40 × 40	1.00 %
6	40 × 40	1.18 %
7	40 × 40	1.76 %
8	40 × 40	1.00 %
9	40 × 40	1.74 %
10	40 × 40	1.06 %
11	40 × 40	1.07 %
12	35 × 35	1.76 %
13	35 × 35	1.60 %
14	30 × 30	3.56 %
15	30 × 30	2.85 %

Declaration of Competing Interest

The authors declare that they have no known competing financial interests or personal relationships that could have appeared to influence the work reported in this paper.

Data availability

Data will be made available on request.

Appendix A. . Initial design results (Eurocode-based)

See Tables A1-A8.

Appendix B. . Optimum design results

See Tables B1-B8.

References

[1] CEN (European Committee for standardisation). Eurocode 8: Design of Structures for Earthquake Resistance-Part 1: General rules, seismic actions and rules for buildings. EN 1998-1-1. Brussels; 2004.
[2] National Standard of the People's Republic of China. Code for seismic design of building (GB50011- 2010). China Architecture and Building Press; 2010.
[3] Council IC. 2021 International Building Code. International Code Council; 2020.
[4] Stevenson JR, Chang-Richards Y, Conradson D, Wilkinson S, Vargo J, Seville E, et al. Organizational Networks and Recovery following the Canterbury Earthquakes. Earthq Spectra 2014;30:555–75. https://doi.org/10.1193/022013EQS041MR.

[5] Meroni F, Squarcina T, Pessina V, Locati M, Modica M, Zoboli R. A Damage Scenario for the 2012 Northern Italy Earthquakes and Estimation of the Economic Losses to Residential Buildings. Int J Disaster Risk Sci 2017;8:326–41. https://doi.org/10.1007/s13753-017-0142-9.

[6] Takeda K, Inaba K. The damage and reconstruction of the Kumamoto earthquake: an analysis on the impact of changes in expenditures with multi-regional input–output table for Kumamoto Prefecture. J Econ Struct 2022;11:20. https://doi.org/10.1186/s40008-022-00276-6.

[7] ASCE/SEI 41-13. Seismic Evaluation and Retrofit of Existing Buildings. 41st–13th ed. Reston, VA: American Society of Civil Engineers; 2014. https://doi.org/10.1061/9780784412855.

[8] Feng D, Kolay C, Ricles JM, Li J. Collapse simulation of reinforced concrete frame structures: Collapse Simulation. Struct Des Tall Spec Build 2016;25:578–601. https://doi.org/10.1002/tal.1273.

[9] Lu Z, Chen X, Lu X, Yang Z. Shaking table test and numerical simulation of an RC frame-core tube structure for earthquake-induced collapse. Earthq Eng Struct Dyn 2016;45:1537–56. https://doi.org/10.1002/eqe.2723.

[10] Moghaddam H, Hajirasouliha I. An investigation on the accuracy of pushover analysis for estimating the seismic deformation of braced steel frames. J Constr Steel Res 2006;62:343–51. https://doi.org/10.1016/j.jcsr.2005.07.009.

[11] Hajirasouliha I, Pilakoutas K. General Seismic Load Distribution for Optimum Performance-Based Design of Shear-Buildings. J Earthq Eng 2012;16:443–62. https://doi.org/10.1080/13632469.2012.654897.

[12] Elnashai AS. Advanced inelastic static (pushover) analysis for earthquake applications. Struct Eng Mech 2001;12:51–69. https://doi.org/10.12989/sem.2001.12.1.051.

[13] ATC. Seismic evaluation and retrofit of concrete buildings-volume 1 (ATC-40). Redwood City, CA: Applied Technology Council; 1996.

[14] FEMA (Federal Emergency Management Agency). Pre-standard and Commentary for the Seismic Rehabilitation of Buildings. Washington, D.C.: FEMA 356; 2000.

[15] Krawinkler H, Miranda E. Part 9: Performance-Based Earthquake Engineering. Earthq. Eng. Eng. Seismol. Perform.-Based Eng., vol. 9, CRC Press; 2004, p. 560–635.

[16] Ghobarah A. Performance-based design in earthquake engineering: state of development. Eng Struct 2001;23:878–84. https://doi.org/10.1016/S0141-0296(01)00036-0.

[17] Mergos PE. Optimum seismic design of reinforced concrete frames according to Eurocode 8 and *fib* Model Code 2010: Optimum Seismic Design of RC Frames According to EC8 and *fib* MC2010b. Earthq Eng Struct Dyn 2017;46:1181–201. https://doi.org/10.1002/eqe.2851.

[18] Foraboschi P. Optimal design of glass plates loaded transversally. Mater Des 2014;1980–2015(62):443–58. https://doi.org/10.1016/j.matdes.2014.05.030.

[19] Chan C-M, Zou X-K. Elastic and inelastic drift performance optimization for reinforced concrete buildings under earthquake loads. Earthq Eng Struct Dyn 2004;33:929–50. https://doi.org/10.1002/eqe.385.

[20] Zou XK, Chan CM, Li G, Wang Q. Multiobjective Optimization for Performance-Based Design of Reinforced Concrete Frames. J Struct Eng 2007;133:1462–74. https://doi.org/10.1061/(ASCE)0733-9445(2007)133:10(1462).

[21] Bai J, Jin S, Zhang C, Ou J. Seismic optimization design for uniform damage of reinforced concrete moment-resisting frames using consecutive modal pushover analysis. Adv Struct Eng 2016;19:1313–27. https://doi.org/10.1177/1369433216642045.

[22] Liu Q, Zhang J, Yan L. An optimal method for seismic drift design of concrete buildings using gradient and Hessian matrix calculations. Arch Appl Mech 2010;80:1225–42. https://doi.org/10.1007/s00419-009-0368-0.

[23] Papazafeiropoulos G, Plevris V, Papadrakakis M. A New Energy-Based Structural Design Optimization Concept under Seismic Actions. Front Built Environ 2017;3:44. https://doi.org/10.3389/fbuil.2017.00044.

[24] Lagaros ND, Papadrakakis M. Seismic design of RC structures: A critical assessment in the framework of multi-objective optimization. Earthq Eng Struct Dyn 2007;36:1623–39. https://doi.org/10.1002/eqe.707.

[25] Fragiadakis M, Papadrakakis M. Performance-based optimum seismic design of reinforced concrete structures. Earthq Eng Struct Dyn 2008;37:825–44. https://doi.org/10.1002/eqe.786.

[26] Gholizadeh S, Salajegheh E. Optimal Design of Structures for Earthquake Loading by Self Organizing Radial Basis Function Neural Networks. Adv Struct Eng 2010;13:339–56. https://doi.org/10.1260/1369-4332.13.2.339.

[27] Arroyo O, Gutiérrez S. A seismic optimization procedure for reinforced concrete framed buildings based on eigenfrequency optimization. Eng Optim 2017;49:1166–82. https://doi.org/10.1080/0305215X.2016.1241779.

[28] Mergos PE. Efficient optimum seismic design of reinforced concrete frames with nonlinear structural analysis procedures. Struct Multidiscip Optim 2018;58:2565–81. https://doi.org/10.1007/s00158-018-2036-x.

[29] Mitropoulou CC, Lagaros ND, Papadrakakis M. Life-cycle cost assessment of optimally designed reinforced concrete buildings under seismic actions. Reliab Eng Syst Saf 2011;96:1311–31. https://doi.org/10.1016/j.ress.2011.04.002.

[30] Razmara Shooli A, Vosoughi AR, MaR B. A mixed GA-PSO-based approach for performance-based design optimization of 2D reinforced concrete special moment-resisting frames. Appl. Soft Comput 2019;85:105843. https://doi.org/10.1016/j.asoc.2019.105843.

[31] Gholizadeh S, Aligholizadeh V. Reliability-based optimum seismic design of RC frames by a metamodel and metaheuristics. Struct Des Tall Spec Build 2019;28:e1552.

[32] Razavi N, Gholizadeh S. Seismic collapse safety analysis of performance-based optimally designed reinforced concrete frames considering life-cycle cost. J Build Eng 2021;44:103430. https://doi.org/10.1016/j.jobe.2021.103430.

[33] Hajirasouliha I, Asadi P, Pilakoutas K. An efficient performance-based seismic design method for reinforced concrete frames: PERFORMANCE-BASED SEISMIC DESIGN OF RC FRAMES. Earthq Eng Struct Dyn 2012;41:663–79. https://doi.org/10.1002/eqe.1150.

[34] Nabid N, Hajirasouliha I, Petkovski M. Adaptive low computational cost optimisation method for performance-based seismic design of friction dampers. Eng Struct 2019;198:109549. https://doi.org/10.1016/j.engstruct.2019.109549.

[35] Mohammadi RK, Garoosi MR, Hajirasouliha I. Practical method for optimal rehabilitation of steel frame buildings using buckling restrained brace dampers. Soil Dyn Earthq Eng 2019;123:242–51. https://doi.org/10.1016/j.soildyn.2019.04.025.

[36] Bai J, Jin S, Ou J. An efficient method for optimizing the seismic resistance of reinforced concrete frame structures. Adv Struct Eng 2020;23:670–86. https://doi.org/10.1177/1369433219878856.

[37] Asadi P, Hajirasouliha I. A practical methodology for optimum seismic design of RC frames for minimum damage and life-cycle cost. Eng Struct 2020;202:109896. https://doi.org/10.1016/j.engstruct.2019.109896.

[38] De Domenico D, Hajirasouliha I. Multi-level performance-based design optimisation of steel frames with nonlinear viscous dampers. Bull Earthq Eng 2021;19:5015–49. https://doi.org/10.1007/s10518-021-01152-7.

[39] Foraboschi P. Bending Load-Carrying Capacity of Reinforced Concrete Beams Subjected to Premature Failure. Materials 2019;12:3085. https://doi.org/10.3390/ma12193085.

[40] Li S, Yu B, Gao M, Zhai C. Optimum seismic design of multi-story buildings for increasing collapse resistant capacity. Soil Dyn Earthq Eng 2019;116:495–510. https://doi.org/10.1016/j.soildyn.2018.10.032.

[41] Arroyo O, Liel A, Gutiérrez S. A Performance-Based Evaluation of a Seismic Design Method for Reinforced Concrete Frames. J Earthq Eng 2018;22:1900–17. https://doi.org/10.1080/13632469.2017.1309605.

[42] Cheng C-T, Chiou S-J, Lee C-T, Tsai Y-B. Study on probabilistic seismic hazard maps of Taiwan after Chi-Chi earthquake. J Geoengin 2007;2:19–28. https://doi.org/10.6310/jog.2007.2(1).3.

[43] Yahya A, Palupi MIR, Suharsono. Seismic Hazard characterization study using an earthquake source with Probabilistic Seismic Hazard Analysis (PSHA) method in the Northern of Sumatra. J Phys Conf Ser 2016;776:012111. https://doi.org/10.1088/1742-6596/776/1/012111.

[44] CEN (European Committee for standardisation). Eurocode 2: Design of concrete structures-Part 1-1: General rules and rules for buildings. EN 1992-1-1. 2004.

[45] Belkacem MA, Bechtoula H, Bourahla N, Belkacem AA. Effect of axial load and transverse reinforcements on the seismic performance of reinforced concrete columns. Front Struct Civ Eng 2019;13:831–51. https://doi.org/10.1007/s11709-018-0513-3.

[46] Yuen TYP, Kuang JS, Kobya V. Influence of Axial Compression Ratio on Drift Capacity of RC Columns 2017:13.

[47] ASCE/SEI 41-06. Seismic rehabilitation of existing buildings. 41st–06 ed. Reston, VA: American Society of Civil Engineers; 2007.

[48] McKenna F, Fenves GL, Scott MH. Computer program OpenSees: open system for earthquake engineering simulation. https://opensees.berkeley.edu.

[49] MATLAB R (2020a). https://uk.mathworks.com/help/matlab/.

[50] ASCE/SEI 41-17. Seismic Evaluation and Retrofit of Existing Buildings. 41st–17th ed. Reston, VA: American Society of Civil Engineers; 2017. https://doi.org/10.1061/9780784414859.

[51] Scott MH, Fenves GL. Plastic Hinge Integration Methods for Force-Based Beam-Column Elements. J Struct Eng 2006;132:244–52. https://doi.org/10.1061/(ASCE)0733-9445(2006)132:2(244).

[52] Mohd Yassin MH. Nonlinear analysis of prestressed concrete structures under monotonic and cyclic loads. Berkeley: Ph.D. University of California; 1994.

[53] Filippou FC, Popov EP, Bertero VV. Effects of bond deterioration on hysteretic behaviour of reinforced concrete joints. of Earthquake Engineering Research Center Report Series 1983;vol. Issue 19.

[54] Neuenhofer A, Filippou FC. Evaluation of Nonlinear Frame Finite-Element Models. J Struct Eng 1997;123:958–66. https://doi.org/10.1061/(ASCE)0733-9445(1997)123:7(958).

[55] CEN (European Committee for standardisation). Eurocode 8: Design of structures for earthquake resistance – Part 3: Assessment and retrofitting of buildings. Brussels; 2016.

[56] Attarchian N, Kalantari A, Moghaddam A-S. CYCLIC BEHAVIOR MODELING OF RECTANGULAR RC BRIDGE PIERS USING OPENSEES. Proc. 4th Int. Conf. Comput. Methods Struct. Dyn. Earthq. Eng. COMPDYN 2013, Kos Island, Greece: Institute of Structural Analysis and Antiseismic Research School of Civil Engineering National Technical University of Athens (NTUA) Greece; 2014, p. 2286–95. https://doi.org/10.7712/120113.4665.C1595.

[57] Calledda C, Montisci A, Porcu MC. Optimal Design of Earthquake-Resistant Buildings Based on Neural Network Inversion. Appl Sci 2021;11:4654. https://doi.org/10.3390/app11104654.

[58] Papageorgiou AS, Halldorsson B, Dong G. TARSCTH (Target Acceleration Spectra Compatible Time Histories) 2002.

[59] Park Y, Ang A-H-S. Mechanistic Seismic Damage Model for Reinforced Concrete. J Struct Eng 1985;111:722–39. https://doi.org/10.1061/(ASCE)0733-9445(1985)111:4(722).

[60] Kappos AJ. Seismic damage indices for RC buildings: evaluation of concepts and procedures. Prog Struct Eng Mater 1997;1:78–87. https://doi.org/10.1002/pse.2260010113.

[61] Powell GH, Allahabadi R. Seismic damage prediction by deterministic methods: Concepts and procedures. Earthq Eng Struct Dyn 1988;16:719–34. https://doi.org/10.1002/eqe.4290160507.

[62] Cosenza E, Manfredi G. Damage indices and damage measures. Prog Struct Eng Mater 2000;2:50–9. https://doi.org/10.1002/(SICI)1528-2716(200001/03)2:1<50::AID-PSE7>3.0.CO;2-S.
[63] Nabid N, Hajirasouliha I, Petkovski M. Performance-based optimisation of RC frames with friction wall dampers using a low-cost optimisation method. Bull Earthq Eng 2018;16:5017–40. https://doi.org/10.1007/s10518-018-0380-2.
[64] Nabid N, Hajirasouliha I, Petkovski M. A Practical Method for Optimum Seismic Design of Friction Wall Dampers. Earthq Spectra 2017;33:1033–52. https://doi.org/10.1193/110316eqs190m.